

# SUPERALLOYS

# 2024

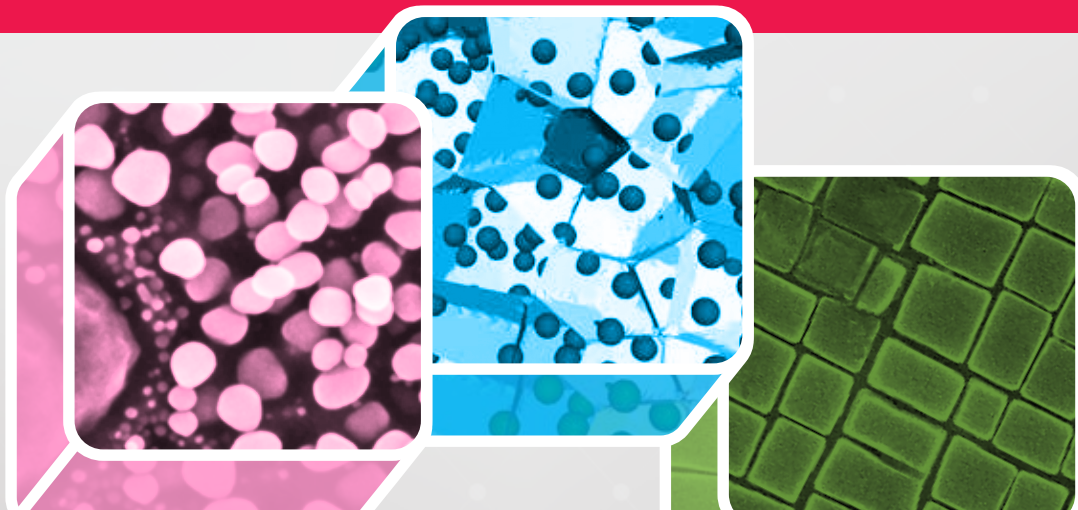


## 15<sup>TH</sup> INTERNATIONAL SYMPOSIUM ON SUPERALLOYS

September 8-12, 2024

Seven Springs Mountain Resort, Champion, Pennsylvania, USA

# PRELIMINARY TECHNICAL PROGRAM



**TMS**

Sponsored by TMS, Structural Materials Division (SMD)  
and the High Temperature Alloys Committee

[www.tms.org/Superalloys2024](http://www.tms.org/Superalloys2024)

---

## Opening Keynote Session

Sunday PM | September 8, 2024  
Exhibit Hall | Seven Springs Mountain Resort

**Session Chairs:** Jonathan Cormier, ENSMA - Institut Pprime - UPR CNRS 3346; Sammy Tin, University of Arizona

---

### 7:30 PM Introductory Comments

#### 7:35 PM Keynote

**Sustainability and Lifecycle Management of Nickel Superalloy Gas Turbine Components:** Ian Edmonds<sup>1</sup>; Stephen Gregson<sup>1</sup>; Neil Glover<sup>1</sup>; Mark Hardy<sup>2</sup>; Ian Mitchell<sup>1</sup>; <sup>1</sup>Rolls-Royce Plc

Nickel-based superalloys remain the essential enabling materials technology for high temperature componentry in gas turbines. Alongside architectural design, nickel alloys have permitted substantial improvement in specific fuel consumption and durability; indeed the Rolls-Royce Ultrafan aero engine is set to be ~25% more fuel efficient than the first generation Trent Engine (Trent 700) and 10% better than the XWB - currently the world's most efficient aero engine [1]. There exists a multitude of complex alloy compositions consciously optimised over 70+ years which have been designed or selected for specific applications. The use of certain constituent elements or processing methods for targeted property improvement must be considered in the context of the full product lifecycle to assess the sustainability trades of new manufacture and through life impact on customer and business value. Original Equipment Manufacturers (OEMs) are now increasingly contracted to deliver 'customer outcomes' rather than just the equipment. The principles of effective Asset Management and Through Life Engineering Services (TES) are discussed and supported by case studies pertaining to lifecycle management, particularly repair methodologies. 'Digital Twins' are a key enabler to optimising the Through Life Engineering Services value levers; understanding/controlling the physics of how superalloys degrade in use is pivotal to delivering better customer, business, and sustainability outcomes. The paper presents a framework for optimising product offerings whilst simultaneously working towards a sustainable future.

---

## General Session 1: Alloy Design/Development I

Monday AM | September 9, 2024  
Exhibit Hall | Seven Springs Mountain Resort

**Session Chair:** Katerina A. Christofidou, University of Sheffield; Paraskevas Kontis, Norwegian University of Science and Technology

---

### 8:30 AM

**"Microstructure Informatics" of Polycrystalline Ni-base Superalloys Using Computer Vision Techniques to Understand Properties and Performance:** Pascal Thome<sup>1</sup>; Luis Arciniaga<sup>1</sup>; Sammy Tin<sup>2</sup>; <sup>1</sup>University of Arizona

Recent advances in hardware technology as well as sophisticated methods for post-processing of Electron Backscatter Diffraction (EBSD) and Energy Dispersive X-Ray Spectroscopy (EDS) data have opened up new possibilities for detailed quantitative microstructure characterization of polycrystalline Ni-based superalloys. However, combining EBSD and EDS scans to reconstruct the true morphology of primary  $\alpha'$  particles remains challenging, as some important microstructural features exist at a scale below the EDS method's lateral resolution limit, which leads to undesired artifacts at  $\alpha/\alpha'$  interfaces. We present an automated computer vision architecture capable of resolving the meso-scale features of polycrystalline  $\alpha/\alpha'$  microstructures with a level of detail that has not previously been demonstrated. Our methodology involves the following steps: 1. The combination of multiple elemental EDS maps. 2. Edge-preserving filtering of EDS maps using a non-local-means algorithm. 3. Unsupervised machine learning phase segmentation based on k-means clustering and 4. An automated artifact correction for the combination of EDS and EBSD information based on morphological conditions. In this manner, digital micrographs are reconstructed in a way that allows for quantitative determination of meaningful numeric metrics by utilizing methods from the field of algorithmic geometry. Various microstructural entities, such as discrete primary  $\alpha'$  particles, mixed  $\alpha/\alpha'$  grains, or  $\alpha$  grains can be characterized separately, including properties of related boundaries. Geometric characteristics can be quantified in terms of the local arrangement and cluster behavior of particle groups, as well as their spacings. The present work contributes to the development of digital workflows for precise and automatic microstructure characterization.

8:55 AM

**Optimizing Local Phase Transformation in Ni-based Superalloys Utilizing Thermodynamically Driven Design Framework and Multiscale Characterization:** *Ashton Egan*<sup>1</sup>; Longsheng Feng<sup>1</sup>; Timothy Smith<sup>2</sup>; Yunzhi Wang<sup>1</sup>; Michael Mills<sup>1</sup>; <sup>1</sup>The Ohio State University; <sup>2</sup>NASA Glenn Research Center

Superalloys are inherently complex alloys to design due to their multicomponent nature; designing alloys to take advantage of the newly discovered Local Phase Transformation (LPT) strengthening creates constraints on alloy composition beyond the conventional considerations for polycrystalline, precipitate-strengthened microstructures. The basis for design is precipitation of  $\pm/\zeta$  on superlattice stacking faults and microtwins while remaining thermodynamically inaccessible to form in bulk. This approach to LPT strengthening has now been demonstrated by optimizing  $\zeta$ -LPT in an empirically designed alloy, NA1, the performance of which is shown here by testing [001] oriented single crystals at several conditions. Computationally designed alloy, NA6, in polycrystalline form, was shown to perform similarly to single crystalline NA1 at 760 °C 552 MPa and outperform single crystal CMSX-4 as well as all LPT-strengthened polycrystalline alloys at this temperature. The deformation substructure of NA6 was investigated via HR-STEM, showing both  $\zeta$ -LPT at SESF as well as  $\pm$ -LPT at microtwins. Compositions of these LPT were elucidated using atomic resolution energy dispersive X-ray spectroscopy and compared to LPT compositions in relevant alloys and discussed considering recent studies on fault propagation velocities.

9:20 AM

**Unambiguous Stacking Fault Analysis for Unraveling Shearing Mechanisms and Shear-based Transformations in the L1<sub>2</sub>-ordered  $\gamma'$  Phase:** Nicolas Karpstein<sup>1</sup>; Malte Lenz<sup>2</sup>; Andreas Bezold<sup>1</sup>; R Zehl<sup>2</sup>; M Wu<sup>1</sup>; Guillaume Laplanche<sup>2</sup>; Steffen Neumeier<sup>3</sup>; *Erdmann Spiecker*<sup>6</sup>; <sup>1</sup>Friedrich-Alexander-Universität Erlangen-Nürnberg; <sup>2</sup>Ruhr-Universität Bochum; <sup>3</sup>University Erlangen-Nuremberg

With its precipitation strengthening effect, the L1<sub>2</sub>-ordered  $\bar{a}$  phase contributes substantially to the mechanical properties of superalloys; therefore, understanding the microscopic mechanisms by which it can be sheared is of key importance. A commonly used method to study these mechanisms involves high-resolution imaging in the transmission electron microscope in <sup>[110]</sup> projection which enables straightforward discrimination between intrinsic and extrinsic stacking faults as well as microtwins. However, the complex or superlattice nature of these stacking fault structures, which provides key information on their formation mechanism, is not necessarily revealed in this projection. In the present work, an experimental approach is presented to resolve this ambiguity and reliably determine the complex or superlattice nature of a stacking fault in the L1<sub>2</sub> structure by additionally imaging the fault in a nearby <sup>[211]</sup> projection, which is achieved by tilting the specimen by 30°. The method is demonstrated using two different application examples in single-crystalline Co-base superalloys. In the first example, the approach enabled the direct experimental verification of two key aspects of the well-known Kolbe mechanism for superlattice extrinsic stacking fault formation, namely the complex nature of the leading intrinsic stacking fault segment and the occurrence of diffusion-mediated re-ordering. In the second example, microscopic details of the shear-based transformation from the cubic L1<sub>2</sub>- $\bar{a}$  to the hexagonal DO<sub>19</sub>- $\bar{c}$  phase are revealed, accounting for additional complexities – again including a re-ordering process – arising from the superlattice ordering of both phases.

9:45 AM

**Effects of Alloying Elements on Twinning in Ni-based Superalloys:** *Valery Borovikov*<sup>1</sup>; Mikhail Mendeleev<sup>1</sup>; Timothy Smith<sup>1</sup>; John Lawson<sup>1</sup>; <sup>1</sup>NASA

Micro-twinning is the major creep deformation mechanism in Ni-based superalloys at temperatures above 700°C. Recent experiments suggest that superlattice stacking faults in  $\gamma$  phase may serve as the precursors to twin formation. Segregation of alloying elements to these precursors may have a significant effect on formation and extension of micro-twins. Using atomistic modeling we investigate and explain the effects of Nb and Cr alloying additions on these processes. The simulation shows that Nb increases the creep resistance which is mostly associated with impeding the reordering of the high energy double complex stacking fault. Cr, on the other hand, promotes twin growth, degrading the high temperature creep properties. These results can help to understand the effects of elemental composition of the alloy on creep resistance.

---

## Interactive Session A: Alloy Design/Development

Monday AM | September 9, 2024

Winterberry | Seven Springs Mountain Resort

---

**A-1: A Novel Wrought Ni-based Superalloy with High-temperature Strength, Resistance to Creep Rupture and Resistance to Oxidation:** *Matthew Bender*<sup>1</sup>; Rafael Rodriguez De Vecchis<sup>1</sup>; Joseph Jankowski<sup>1</sup>; <sup>1</sup>ATI

ATI 273™ alloy was developed to be a fabricable, creep-resistant, and oxidation-resistant superalloy. This paper summarizes material characterization of early vacuum-melted lab heats focusing primarily on its oxidation resistance, though high-temperature strength properties will also be addressed. Short- and long-term continuous isothermal exposure data for 871 and 982 °C testing in dry air will be presented with an emphasis on understanding the impact of Ta addition on scale formation. Furthermore, cyclic exposure testing in flowing air was carried out to assess oxide scale adhesion and healing. ATI 273 has an intentional tantalum addition of 2.5 wt. %, and this impactful element increases the alloy's resistance to both oxidation and creep. This paper will show the alloy's improved properties are linked to Ta addition and Ti reduction in the chemistry leading to improved properties compared to ATI 263™ and Haynes® 282® alloys. ATI 273 is being considered for high temperature structural applications, especially those for land-based gas turbine and aerospace engines.

**A-2: Accelerating Alloy Development for Additive Manufacturing:** *Elisabeth Kammermeier*<sup>1</sup>; *Julius Weidinger*<sup>1</sup>; *Illya Ionov*<sup>1</sup>; *Markus Ramsperger*<sup>2</sup>; *Benjamin Wahlmann*<sup>1</sup>; *Carolin Körner*<sup>1</sup>; *Christopher Zenk*<sup>1</sup>; <sup>1</sup>Fau Erlangen-Nuernberg, Wtm; <sup>2</sup>GE Additive

Additive Manufacturing (AM) is revolutionizing the production of complex superalloy parts, yet its advancement is hindered by the high costs and extensive time required for atomizing powders from which new alloys are produced and tested. This study presents our approach to expedite and economize alloy development for AM. At the heart of this method is the CALPHAD-based multi-criteria optimization algorithm PyMultOpt, utilized for selecting potential alloys, which are then produced through arc-melting. Our innovative testing framework involves two key processes: (i) assessing alloy processability via electron beam remelting of bulk material, and (ii) evaluating mechanical properties after refining coarse-grained material via deformation and recrystallization. Focusing on Alloy 247 and derivatives selected through PyMultOpt, our approach successfully emulates AM-like microstructures in arc-melted material. The compressive creep tests on the recrystallized microstructure of Alloy 247 indicate a minimal creep rate comparable to that of AM specimens. Moreover, profilometry-based indentation plastometry tests at 760 °C offer a rapid, high-temperature evaluation method, allowing for preliminary alloy ranking before extensive creep testing. This study demonstrates that remelting and recrystallization of bulk material can reproduce AM-like microstructures, enabling a faster and more cost-effective assessment and ranking of new alloys in terms of their mechanical properties and AM-processability, as opposed to the traditional, powder-dependent alloy development methods.

**A-3: Composition and Heat Treatment Modifications of a New Low-cost Ni Base Wrought Alloy for Improved Creep Resistance and Elevated Temperature Ductility:** *Ning Zhou*<sup>1</sup>; *Filip Van Weereld*<sup>1</sup>; *Gian Colombo*<sup>1</sup>; *Mario Epler*<sup>1</sup>; <sup>1</sup>Carpenter Technology Corporation

Exp-G27 is a new low-cost Ni base wrought alloy developed by Carpenter Technology Corporation for applications such as jet engine turbine casing and internal combustion engine exhaust valves. Mainly strengthened by  $\alpha'$ , Exp-G27 has higher temperature stability compared to alloy 718. Within the targeted service temperature range between 704 °C to 871 °C, Exp-G27 demonstrates comparable mechanical performance as Waspaloy but with a significantly lower raw material cost. However, the creep and stress rupture of Exp-G27 is slightly lower than Waspaloy. In this study, a cost-performance tradeoff study was carried out to help make modification to the original Exp-G27 to achieve superior creep/stress rupture performance than Waspaloy while still being cost competitive.

**A-4: Development of a New Low-cost Polycrystalline Nickel-base Superalloy:** *George Wise*<sup>1</sup>; *Hon Tong Pang*<sup>1</sup>; *Paul Mignanelli*<sup>2</sup>; *Mark Hardy*<sup>2</sup>; *Nicholas Jones*<sup>1</sup>; *Howard Stone*<sup>1</sup>; <sup>1</sup>University of Cambridge; <sup>2</sup>Rolls-Royce plc

There is significant industrial demand for low-cost polycrystalline Ni-base superalloys that can be utilised for rotating and static applications at intermediate temperatures in aircraft engines. In this work, we report on the microstructure, heat treatment response, mechanical properties and oxidation behaviour of a newly developed alloy for these applications. The alloy has been designed to improve on the thermal stability and mechanical performance of Inconel718 (IN718), whilst offering lower processing costs than advanced cast & wrought alloys such as Alloy 720Li and Renè 65. The study highlights key areas of alloy development, comparing the alloy properties where possible to current commercially available alternatives.

**A-5: Development of Novel Ni-Co Base P/M Disk Superalloy by Redesigning Based on Turbine Blade Alloy, TM-47:** *Toshio Osada*<sup>1</sup>; *Makoto Osawa*<sup>1</sup>; *Yuhi Mori*<sup>1</sup>; *Ayako Ikeda*<sup>1</sup>; *Hiroshi Harada*<sup>1</sup>; *Takuma Kohata*<sup>1</sup>; *Kyoko Kawagishi*<sup>1</sup>; <sup>1</sup>National Institute for Materials Science

The temperature capability of current state-of-the-art high-pressure disk superalloys is around 700°C. To further improve their temperature capabilities, new disk alloy design approaches with a focus on blade alloy compositions, which was designed for applications at temperatures of above 900°C or higher, may be effective. In this study, novel Ni-Co base disk superalloys were designed based on a combination of Ni-base blade superalloy TM-47 and Co-12.5wt.% Ti, both of which possess a  $\gamma$ - $\gamma'$  two-phase structure. First screen results using single crystal casts revealed TM-47 to be a potentially promising candidate as a base alloy for Ni-Co base disk superalloy, while additions of Co-12.5 wt.% Ti to TM-47 was found to improve creep strength of the alloy. A later investigation using P/M alloys revealed that limited additions of Co-12.5wt.% Ti to the base alloy also improves powder manufacturability, phase stability, and high temperature proof stress. Thus, TM-47 M2 (20 wt.% addition of Co-12.5wt.% Ti to TM-47) was selected as a candidate alloy for subscale manufacturing trial. Creep tests at 760 °C/630MPa demonstrated that the selected TM-47 M2 provides superior creep properties compared to other conventional disk superalloys, especially for the 0.2 % creep time, which is a critical property for high pressure turbine disks.

**A-6: Effect of the Interfacial Strain Anisotropy on the Raft Structure of Ni-base Single Crystal Superalloys and Novel Alloy Design Approach by Controlling the Lattice Misfit and the Elastic Misfit:** *Takuma Saito*<sup>1</sup>; *Hiroshi Harada*<sup>2</sup>; *Tadaharu Yokokawa*<sup>2</sup>; *Makoto Osawa*<sup>1</sup>; *Kyoko Kawagishi*<sup>1</sup>; *Shisuke Suzuki*<sup>2</sup>; <sup>1</sup>National Institute for Materials Science; <sup>2</sup>Waseda University

Enhancing the aspect ratio of the precipitates in the raft structure of Ni-base single crystal superalloys for high-pressure turbine blades is a fundamental approach to improve the creep resistance at higher temperature and lower stress conditions. To obtain larger aspect ratio, the alloy design strategy to enlarge the lattice misfit between and phases towards negatively larger side has been applied. However, the fundamental driving force for the raft structure formation, "interfacial strain anisotropy", has been ignored for the alloy design. Here, interfacial strain anisotropy is a difference of the interfacial strain between horizontal and vertical / interface, and this is caused by the interaction of loading stress with the elastic misfit between and phases. In this study, model alloys imply that the aspect ratio is modulated by kinetic factor caused by Re with a presence of interfacial strain anisotropy.

**A-7: Effects of Zirconium Additions on the Microstructure and Stress-rupture Properties in Polycrystalline Ni-base Superalloys:** *Yang Zhou*<sup>1</sup>; *Yanna Cui*<sup>1</sup>; *Bo Wang*<sup>1</sup>; *Jiamiao Liang*<sup>1</sup>; *Shuping Li*<sup>1</sup>; *Jun Wang*<sup>1</sup>; <sup>1</sup>Shanghai Jiao Tong University

In present work, comprehensive investigations were conducted to examine the distribution behavior of the minor alloying element Zr, its impact on microstructural evolution and effect on the high-temperature stress-rupture properties in IN 100 superalloys. The results indicate that the presence of Zr influences the eutectic phase in as-cast alloys, resulting in a reduction in the  $\alpha$  channel width and an increase in both the volume fraction and size of the  $\alpha'$  phase. Through time of flight-secondary ion mass spectrometry and transmission electron microscope analysis, Zr is found to segregate along the eutectic front in the form of Ni5Zr in 900 °C stress-ruptured samples, rendering IN 100 alloys enhanced creep resistance at elevated temperatures. Heat treatment at 1200 °C could effectively eliminate the eutectic structure, thus mitigating the segregation of Zr. A maximum endurance life in IN 100 alloys at 900 °C /314 MPa and 950 °C /225 MPa is reached when Zr content is approximately 700 ppm. Synergistic effects including the eutectic content, volume fraction and the degree of rafting of the  $\alpha'$  phase together with the dislocation network structure were analyzed and discussed, contributing to the improved stress-rupture properties in IN 100 alloys.

**A-8: Enhancing Economic Affordability of Aircraft Engines: Development of a Low-cost Single Crystal Superalloy DD93 Containing 3 wt.% Re, Designed to Meet Third Generation Superalloys Properties:** Yongmei Li<sup>1</sup>; Zihao Tan<sup>1</sup>; Haoyu Guo<sup>2</sup>; Xinguang Wang<sup>1</sup>; Jinguo Li<sup>1</sup>; Yizhou Zhou<sup>1</sup>; Xiaofeng Sun<sup>1</sup>; <sup>1</sup>Institute of Metal Research, Chinese Academy of Sciences

Developing novel and affordable Ni-based single crystal (SC) superalloys is crucial in order to address the escalating expense of advanced industrial aero engines. The present work introduces a novel low-cost SC superalloy DD93, designed to meet the performance requirements of third-generation superalloys, which have a Re content of only 3 wt.%. The alloy design proceeded focusing on reducing the Re addition whilst still maintaining a high temperature capability at 1120°. Comprehensive performance tests confirmed that DD93 has great microstructural stability, and its stress rupture properties and tensile strength are comparable to those of commercial third-generation SC superalloys. In addition, DD93 was evaluated and shown to have favorable fatigue strength, environmental resistance, coating compatibility and castability. More importantly, the reduced Re content of 3 wt.% leads to a considerable cost reduction of almost 40 % compared to CMSX-10 and René N6. The competitiveness of DD93 in terms of cost and mechanical properties improves the affordability of turbine blades and shows promising prospects for its application in advanced aero-engine turbine blades.

**A-9: Freckle Formation Propensity Criterion for New Superalloy Design:** Adarsh Shukla<sup>1</sup>; Richard DiDomizio<sup>2</sup>; Andrey Meshkov<sup>2</sup>; Timothy Hanlon<sup>2</sup>; Daniel Cody<sup>2</sup>; <sup>1</sup>GE Aerospace Research, India; <sup>2</sup>GE Aerospace Research, USA;

Freckles are casting anomalies generally detrimental to the mechanical properties of superalloys. This work presents a new freckle formation propensity criterion calculated using only alloy composition to rank the freckle propensity of alloys when processed via the same melting route at common conditions. This is achieved by combining literature established changes in density of solidifying liquid ( $\rho/\rho$ ) with an approximation for permeability within the mushy zone, using enthalpy of fusion and solidification range of the alloy. Also, a methodology to calculate  $\rho/\rho$  using electron probe microanalysis (EPMA) on as-cast coupons of superalloys is outlined. Additional factors influencing the permeability within the mushy zone, such as the presence of primary carbides, can also be calculated based on alloy chemistry, and incorporated to refine the freckle formation propensity criterion.

**A-10: Microstructural and Thermomechanical Assessment of Computationally Designed Ni-based SX Superalloys:** Abel Rapetti<sup>1</sup>; Alice Cervellon<sup>1</sup>; Edern Menou<sup>2</sup>; Jérémy Rame<sup>3</sup>; Franck Tancret<sup>4</sup>; Jonathan Cormier<sup>1</sup>; Paraskevas Kontis<sup>5</sup>; <sup>1</sup>Institut Pprime Upr Cnrs 3346; <sup>2</sup>Safran Tech; <sup>3</sup>Safran Aircraft Engines; <sup>4</sup>Institut des Matériaux Jean Rouxel - UMR 6502; <sup>5</sup>Norwegian University of Science and Technology

Five computationally designed single crystal superalloys have been developed for aircraft engine airfoils submitted to high temperatures. The broad steps of the alloy design procedure are presented in this study. Tensile and creep properties of these SX superalloys are evaluated in regard to the predictions of the creep-life model and/or in regard with reference SX superalloys. Effective and predicted density show a good consistence. The  $\bar{\alpha}$ ' phase fraction predicted by CALPHAD calculations at the design stage and the ones evaluated in this work are consistent as well. For AMSP2 alloy, atom probe tomography measurements were conducted. We observe that excessive additions of rhenium to a platinum containing SX superalloy have a strong impact on creep properties, reducing the creep lifetime compared to the reference alloy TROPEA, and strongly affect the  $\bar{\alpha}/\bar{\alpha}$ ' coherency, leading to the absence of rafting at intermediate temperatures (950 °C – 1050 °C).

**A-11: Principle for Homogenization Design of High-generation Single Crystals Superalloys Containing Increased Refractory Contents:** Wanshun Xia<sup>1</sup>; Xinbao Zhao<sup>1</sup>; Quanzhao Yue<sup>1</sup>; Yuefeng Gu<sup>1</sup>; Ze Zhang<sup>1</sup>; <sup>1</sup>Zhejiang University

Increasing the fractions of certain refractory elements resulted in the development of modern single-crystal superalloys with improved high-temperature performance, but also increased solidification segregation of elements. The importance of solution treatment to reduce segregation and homogenize the microstructure has been well verified; however, guidelines for achieving simple but effective homogenization practices have yet to be developed. In this study, the effects of different solution treatments on the creep properties of a fourth-generation single-crystal superalloy were investigated, and two guidelines for designing homogenization practices for modern single-crystal superalloys were proposed. First, the degree of homogenization achieved by solution treatment will be saturated once the dendritic segregation coefficient of specific elements reaches a certain limit (lower than 1.2 for Re and W, and higher than 0.9 for Al and Ta). Second, if the residual segregation is strong, different degrees of local deformations between the dendrite core (D) and interdendritic (ID) regions induce uneven fractures in the alloy. An effective, fully homogenized structure should exhibit similar local strengths in the D and ID regions. These guidelines will help assess the effectiveness of solution treatments and guide the development of new solution treatment strategies for modern single-crystal superalloys.

---

## General Session 2: Alloy Design/Development II

Monday AM | September 9, 2024  
Exhibit Hall | Seven Springs Mountain Resort

**Session Chair:** Tresa M. Pollock, University of California - Santa Barbara ; Akane Suzuki, GE Aerospace Research

---

11:20 AM

**Computational Design and Experimental Characterization of a Novel 3rd Generation Single Crystal Superalloy with Balanced High Temperature Creep Strength and Corrosion Resistance:** Jeremy Rame<sup>1</sup>; Edern Menou<sup>2</sup>; Didier Locq<sup>3</sup>; Yohan Cosquer<sup>4</sup>; Amar Saboundji<sup>2</sup>; Mikael Perrut<sup>3</sup>; <sup>1</sup>Safran Aircraft Engines, NAAREA; <sup>2</sup>Safran Tech; <sup>3</sup>DMAS, ONERA, Université Paris-Saclay; <sup>4</sup>DGA Techniques aéronautiques

This paper presents the development of AMS20, a novel third-generation single crystal superalloy designed for the next generation of aeroengines. The alloy design utilizes a computational approach that combines empirical models and CALPHAD calculations to identify compositions meeting targeted specifications. This methodology facilitates the selection of the final AMS20 alloy composition, aiming to optimize high temperature creep properties while preserving excellent high temperature oxidation resistance. The alloy was cast and single crystal bars were grown using the conventional Bridgman method. Subsequently, appropriate solution and aging treatments were developed, and the tensile and creep properties of AMS20 were evaluated. A comparative analysis was performed against reference second and third-generation single crystal superalloys, namely CMSX-4, CMSX-10K, CMSX-4 Plus, and AGAT. Results indicate that AMS20 exhibits a remarkable combination of high temperature creep and oxidation resistance. Specifically, AMS20 demonstrates a creep life at 1200 °C comparable to CMSX-10K alloy, while its cyclic oxidation performance at 1150 °C is akin to second-generation CMSX-4 alloy and notably superior to third-generation reference alloys. However, it is important to note that initial aging results highlight the sensitivity of AMS20 alloy to TCP phases at 1050 °C and its relatively narrow high temperature processing windows. Yet AMS20 remains a promising single crystal superalloy for the future generation of aircraft engines.

11:45 AM

**On the Evolution of the  $\gamma$ - $\gamma'$  Lattice Misfit and TCP Phase Precipitation in a Highly Alloyed Single Crystalline Ni-base Superalloy:** Jakob Bandorf<sup>1</sup>; Anna Kirzinger<sup>1</sup>; Christopher Zenk<sup>1</sup>; Hon Tong Pang<sup>2</sup>; Catherine Rae<sup>2</sup>; Howard Stone<sup>2</sup>; Steffen Neumeier<sup>1</sup>; <sup>1</sup>Friedrich-Alexander-Universität Erlangen-Nürnberg; <sup>2</sup>University of Cambridge

Ni-base superalloys of the latest generation are prone to the formation of topologically close-packed (TCP) phases due to their high content of refractory elements. The quantitative correlation between the TCP phase precipitation, the evolution of the lattice parameters, and the  $\gamma$ - $\gamma'$  lattice misfit in a highly alloyed single crystal Ni-base superalloy is investigated here. Even in the standard heat-treated state TCP phases are found in the dendrite cores. With additional annealing at 1100 °C further TCP phase precipitation occurs until a constant fraction is reached after 100 h. High-resolution X-ray diffraction experiments conducted at room temperature revealed that the lattice parameter of the  $\gamma$  phase decreases with increasing exposure time and reaches, like the TCP phase fraction, a kind of plateau after long aging durations. In contrast, the lattice parameter of the  $\gamma'$  phase hardly changes throughout aging, which results in a decrease of the initial  $\gamma$ - $\gamma'$  lattice misfit from about -1 % to a plateau of about -0.45 % after 1000 h. Comparison of thermodynamic and lattice parameter calculations with the experimentally determined values revealed that the depletion of the main TCP phase forming elements Re, W and Mo associated with the ongoing TCP phase formation is the main reason for this behavior. It is also shown that the effect of both stress relaxation and TCP phase precipitation results in a reduction of the tetragonal distortion and coherency stresses in the  $\gamma$  matrix channels.

12:10 PM

**Combinatorial Materials Research for the Development of New Advanced CoNi-base Superalloys:** Lukas Haussmann<sup>1</sup>; Steffen Neumeier<sup>1</sup>; Andreas Hausmann<sup>1</sup>; Enrico Bergamaschi<sup>1</sup>; Mathias Goeken<sup>1</sup>; <sup>1</sup>Fau Erlangen-Nuernberg

Nanomechanical testing methods are very well suited to complement combinatorial materials research using diffusion couples. Diffusion couples allow the investigation of the microstructure and the mechanical properties of multiple alloy compositions in a single sample without the need to cast many different alloys. To expand the investigation of mechanical properties on diffusion couples to higher temperatures, indentation creep is a highly suitable technique. In this work, the diffusion couple approach was utilized in combination with a high temperature indentation creep testing technique, using a 25  $\mu$ m flat punch indenter, to conduct combinatorial investigations on a Co-Ni diffusion couple and on a multinary  $\gamma$ /CoNiCr-base superalloy diffusion couple with increasing Cr content. For the Co-Ni system, the highest room temperature hardness and highest creep resistance at 550 °C was observed between 50 at.% Co to 80 at.% Co. For the  $\gamma$ /CoNiCr-base superalloy CoWAlloy2, an optimum Cr content of 14 at.% has been found. Up to this Cr content the hardness and creep resistance is not altered and the precipitation of undesired phases does not occur. With further increasing Cr content, the volume fraction decreases significantly and undesired W- and Al-rich phases precipitate, leading to an increase in hardness but a deterioration of the creep properties.

12:35 PM

**Influence of Re on High-temperature Microstructural Stability and Mechanical Properties of High-Cr CoNi-based Superalloys:** Xiaorui Zhang<sup>1</sup>; Longfei Li<sup>1</sup>; Song Lu<sup>1</sup>; Muchun Hou<sup>1</sup>; Min Zou<sup>1</sup>; Qiang Feng<sup>1</sup>; <sup>1</sup>University of Science and Technology Beijing

A multicomponent high-Cr CoNi-based superalloy was developed for potential use in industrial gas turbine materials. In response to the enhanced overall performance of alloys, the microstructural stability and strength of alloys with different Re additions at 950 °C were investigated. During long-term thermal exposure, the  $\bar{\alpha}$  precipitates remained nearly cuboidal and the addition of Re led to a mild decrease in the  $\bar{\alpha}$  volume fraction. The Re addition can effectively reduce the coarsening rate of  $\bar{\alpha}$  precipitates due to both the significant reduction in the effective diffusion coefficient in the  $\bar{\alpha}$  matrix and the decrease in interfacial energy between the  $\bar{\alpha}$  and  $\alpha$  phases. Despite a reduction in  $\bar{\alpha}$  volume fraction, the addition of Re improved the creep properties of the investigated alloys at 950 °C/200 MPa - 300 MPa. Firstly, the introduction of Re causes the inversion of W partitioning from  $\bar{\alpha}$  matrix to  $\bar{\alpha}$  precipitates to improve the  $\bar{\alpha}$  strength. And it also elevates the content of Re within the  $\bar{\alpha}$  phase, thereby enhancing the solid solution strengthening effect. Moreover, this improvement is also attributed to a decrease in the effective diffusion coefficient of the alloy. All these factors contribute to improving the creep properties and yield strength of high-Cr CoNi-based superalloys.

---

### General Session 3: Disk Alloy Mechanical Behavior I

Monday PM | September 9, 2024

Exhibit Hall | Seven Springs Mountain Resort

**Session Chairs:** Mark Hardy, Rolls-Royce Plc; Nicholas Krutz, PCC Metals

6:00 PM

**Inhomogeneous Distribution and Coarsening of  $\gamma''$  Precipitates in a Ni-based Superalloy and their Effect on Creep:** Chang-Yu Hung<sup>1</sup>; Stoichko Antonov<sup>1</sup>; Paul Jablonski<sup>1</sup>; Martin Detrois<sup>1</sup>; <sup>1</sup>National Energy Technology Laboratory

Modifications to INCONEL® alloy 725 (IN725) with higher Nb or Ta and high Ti/Al ratio previously revealed the formation of  $\gamma''$  precipitates as the sole precipitate strengthening phase which was accompanied with significant increases in elevated temperature strength and resistance to creep deformation. In this study, the  $\gamma''$  alloys (named M725-Nb and M725-Ta) were chosen to observe the microstructural evolution of  $\gamma''$  precipitates during creep. Following aging,  $\gamma''$  was found to be the main precipitate strengthening phase with no detectable  $\gamma'$  in both M725 alloys. After creep, the grip/gage sections of the crept M725-Nb/Ta exhibited preferential coarsening and inhomogeneous distribution of  $\gamma''$  platelets, and sandwich-like structures, comprising of cubic  $\gamma'$  precipitates with small  $\gamma''$  discs on each facet. This  $\gamma''$  variant selection behavior taking place in the grip section with no stress applied was different from the typical stress-induced variant selection reported in previous literature. However, creep tested specimens with prior high temperature exposure to promote varying  $\gamma''$  characteristics prior to deformation demonstrated a similar creep behavior when compared to aged specimens tested under identical conditions. This suggested that the coarsening and inhomogeneous distribution of  $\gamma''$  precipitates was not the determinant factor for creep life in bulk M725-Nb/Ta alloys. The failure of bulk M725 was linked with the development of cracks along grain boundaries (GBs), where the emergence of Nb-rich  $\delta$  and/or Ta-rich  $\delta$  phases at the GB markedly depleted the  $\gamma''$  strengthening phase in the surrounding GB regions which led to localized weakening.

6:25 PM

**Spark Plasma Sintering of Nickel-based Superalloys: A New Route to Produce Dual-alloy Turbine Disks:** *Emmanuel Saly*<sup>1</sup>; Patrick Villechaise<sup>2</sup>; David Mellier<sup>1</sup>; Pierre Sallot<sup>2</sup>; Amélie Caradec<sup>1</sup>; Jonathan Cormier<sup>1</sup>; <sup>1</sup>ENSMA - Institut Pprime - UPR CNRS 3346; <sup>2</sup>Safran Tech

Spark Plasma Sintering was used to join powders of two nickel-based superalloys containing over 40% volume fraction of  $\gamma'$  phase and considered very difficult to weld. After one minute of sintering, a very high relative density was reached, and both alloys were successfully solid-state joined without precipitation of detrimental phases in the diffusion-affected zone. Solutioning of samples showed that a dual-alloy-microstructure, composed of a coarse-grained alloy in the rim and a fine-grained alloy in the core, could be produced by this technique. In both as-received and fully-heat-treated states, assemblies exhibit tensile strengths at least higher than the weakest parent material. The heat-treatment sequence enables modulating strain partitioning during tension, leading to a more homogeneous deformation at very high stresses. Thus, failure occurs in the weakest parent material, far from the weld, with no alteration of the ductility, suggesting a sound joint has been produced during the short sintering time. The study on the viscoplastic response by means of tensile stress relaxation tests shows that a dual-alloy disk technology has a high potential, resulting in improved creep properties, chemical stability, and corrosion resistance in the rim section.

6:50 PM

**Viscoplastic Behavior of the Grain Size Transition Zone in a Dual Microstructure Turbine Superalloy Disk:** *Fabio Machado Alves da Fonseca*<sup>1</sup>; Denis Bertheau<sup>2</sup>; Loïc Signor<sup>2</sup>; Julien De Jaeger<sup>3</sup>; Patrick Villechaise<sup>2</sup>; Jonathan Cormier<sup>2</sup>; <sup>1</sup>SafranTech/Institut PPrime; <sup>2</sup>Institut PPrime; <sup>3</sup>Safran Tech

This study focuses on the challenging characterization of the microstructures and the viscoplastic behavior (creep, relaxation) within the transition region of dual microstructure disks made of  $\gamma$ - $\gamma'$  Ni-based superalloys. This transition microstructure, consisting in spatial variations of grain sizes and/or  $\gamma'$  precipitation, poses difficulties in providing insights for effective modeling strategies in aero-engines. To characterize viscoplastic behavior at intermediate temperatures, stress relaxation tests were employed using AD730TM superalloy. A single-crystalline version of AD730™ was used to isolate the effects of different precipitation states (ranging from 15 to 300 nm in size), at 700 °C and 800 °C. The results reveal a significant impact at 700 °C, while no substantial impact was observed at 800 °C. Additionally, precise specimen machining was conducted in different radial zones of a dual disk to explore the influence of various grain size gradients, on viscoplastic behavior at both 700 °C and 800 °C. The findings indicate a progressive viscoplastic behavior along the gradient of grain size for both testing temperatures. Finally, the viscoplastic behavior of transition specimens was analyzed within the framework of a grain-sensitive phenomenological model. The study provides valuable insights into understanding and modeling the complex behavior of dual microstructure disks in aero-engine applications.

## Interactive Session B: Disk Alloy Mechanical Behavior

Monday PM | September 9, 2024

Winterberry | Seven Springs Mountain Resort

**B-1: Effect of Grain Boundary Serrations on Creep Deformation of Udimet-720Li Superalloy:** *Tso-Wei Chen*<sup>1</sup>; Po-Cheng Wu<sup>2</sup>; Hideyuki Murakami<sup>3</sup>; Yoshiaki Toda<sup>3</sup>; An-Chou Yeh<sup>1</sup>; Yung-Chang Kang<sup>4</sup>; <sup>1</sup>National Tsing Hua University; <sup>2</sup>S-Tech Corporation; <sup>3</sup>National Institute for Materials Science; <sup>4</sup>Gloria Material Technology Corporation

This article investigates grain boundary serration and its effects on high-temperature creep behavior of Udimet-720Li. Grain boundary serration is induced by controlled cooling during heat treatments, with continuous and discontinuous precipitation of  $\gamma'$  phase identified as the competing mechanisms affecting serration formation. Continuous precipitation of coarse  $\gamma'$  particles pin grain boundaries and leads to a slight serration termed the continuous precipitation type (type-I) boundary, while discontinuous reaction forming cellular  $\gamma/\gamma'$  behind the mobile grain boundary causes larger serration known as the discontinuous precipitation type (Type-II) boundary. Samples with straight (STB), Type-I (SRB-1), Type-II (SRB-2) grain boundaries were produced, and creep behaviors under 700 °C/700MPa were investigated.

**B-2: Effect of Non-fully Recrystallized Grain Structures on the Fatigue Behavior of a Wrought  $\gamma$ - $\gamma'$  Ni-base Superalloy:** *Linhan Li*<sup>1</sup>; Ji Zhang<sup>1</sup>; Ran Duan<sup>1</sup>; Kangkang Liu<sup>1</sup>; Qiang Tian<sup>1</sup>; Wenyun Zhang<sup>1</sup>; Zhongmin Shen<sup>1</sup>; Beijiang Zhang<sup>1</sup>; <sup>1</sup>China Iron & Steel Research Institute Group

The effect of non-fully recrystallized (NFRX) microstructures on the fatigue performance of  $\gamma$ - $\gamma'$  Ni-base superalloy GH4065A was investigated by comparing the fatigue properties of specimens with a homogeneous fine-grained structure and a heterogeneous grain structure containing many NFRX regions. The fatigue life was characterized by performing strain-controlled fatigue tests at 500° with a maximum strain amplitude  $\Delta\varepsilon_{\max}/2$  ranging from 0.8% to 0.45%. In order to study the fatigue slip, crack initiation and propagation behaviors associated with the NFRX structures, interrupted stress-controlled fatigue tests of dog-bone shape specimens were carried out at 400°, employing two loading levels with the maximum stress amplitude  $\Delta\sigma_{\max}$  above and below the yield strength, respectively. The NFRX grain structures were characterized and classified into two distinct types: unrecrystallized (URX) and partially recrystallized (PRX). Their effect on the slip bands formation, crack initiation and propagation were investigated and compared with that of the fully recrystallized (FRX) structure. The superior resistance of NFRX structures to the fatigue damage, particularly restricting slip-induced crack initiation and inclusion-induced crack propagation, makes the FRX regions accumulate most of the fatigue damage, resulting in unnoticeable variation in fatigue life.

**B-3: How Can the Non-metallic Inclusions Distribution Lead to an Anisotropy in the Fatigue Life Durability of Forged  $\gamma$ - $\gamma'$  Ni-based Disks Alloys?** *Adèle Govaere*<sup>1</sup>; Moubine Al-Kotob<sup>1</sup>; Xavier Baudequin<sup>1</sup>; Caitline Lasne<sup>1</sup>; Romain Lambert<sup>1</sup>; Jonathan Leblanc<sup>1</sup>; Arnaud Longuet<sup>1</sup>; Nicolas Sutter<sup>1</sup>; Alexia Wu<sup>1</sup>; Jonathan Cormier<sup>2</sup>; Azdine Nait-Ali<sup>2</sup>; Malo Prié<sup>2</sup>; <sup>1</sup>Safran Aircraft Engines; <sup>2</sup>Institut Pprime, ISAE-ENSMA

The impact of non-metallic inclusions (NMIs) and the forging process on the low-cycle fatigue (LCF) durability of a  $\gamma$ - $\gamma'$  superalloy is investigated. X-ray synchrotron tomography was performed to characterize the NMIs populations. Low cycle fatigue was tested at 400 °C on specimens taken in various orientations on forged disks using the ring rolling process or the die forging one. The results show anisotropic tensile and fatigue properties for the ring rolled disks, especially in radial and axial directions. On the other hand, no reduction of the lifespan was observed for the die forged ones. Fractographic observations and a macroscopic approach in modelling of a particle during forging were conducted. It showed that abnormal low lifetimes are connected to crack initiation at NMIs. However, it is not a sufficient condition. The length of NMIs stringers and their orientation in the disk are important parameters. The forging process has a strong impact on the plastic flow and the initial state of the particles. Indeed, ring rolling promotes decohesion at the interface between the inclusion and the matrix. The crack initiation time and the first stages of the propagation to the matrix highly contribute to low lifespan. A better understanding of the detrimental configurations of NMIs would allow optimized forging processes.

**B-4: Improvement in Mechanical Properties of Ni-base Superalloy Alloy247 Using Hot Forging:** *Shintaro Yoshimoto*<sup>1</sup>; Yuhi Mori<sup>1</sup>; Masahiro Hayashi<sup>1</sup>; Takashi Shibayama<sup>2</sup>; Takeshi Izumi<sup>2</sup>; Yinya Imano<sup>2</sup>; <sup>1</sup>Honda R&D Co.,Ltd.; <sup>2</sup>Mitsubishi Heavy Industries Ltd.,

To improve the low-cycle fatigue (LCF) strength of Alloy247, refinement of the alloy microstructure through the forging process has been trialed and the mechanical properties and microstructure of the forged alloy were compared with that of the conventional casted alloy. By utilizing the MH (Mitsubishi Hitachi) process, an ingot of Alloy247 with high volume fraction of  $\gamma'$  phase was successfully forged without cracking. In contrast with cast Alloy 247, forged Alloy247 exhibited uniform microstructure with  $\gamma'$  precipitates, the grain size was significantly reduced from 10mm in the cast alloy to 200 mm in the forged alloy, and the eutectic structure was eliminated completely. Results obtained from high temperature tensile testing showed remarkable improvement in elongation which led to higher ultimate tensile strength (UTS) values. Owing to the fine microstructure, forged Alloy247 showed 15 times longer LCF life than that of the cast alloy although creep strength slightly decreased in low stress regions. Significant improvement in LCF life of Alloy247, which has intrinsically high creep strength, allows for tuning of the mechanical properties based on requirements and broadens the application of the alloy to hot section parts.

**B-5: Low-cycle Fatigue Performance and Associated Deformation Mechanisms of HAYNES 244 Alloy and Waspaloy:** Michael Fahrman<sup>1</sup>; Michael Titus<sup>2</sup>; *Thomas Mann*<sup>1</sup>; <sup>1</sup>Haynes Intl.; <sup>2</sup>Purdue University

One key performance attribute of cases and seals in advanced gas turbine engines is resistance to thermal fatigue, which is dictated by strains associated with thermal cycling of the component and the material's intrinsic resistance to fatigue crack initiation and propagation. Frequently isothermal strain-controlled low-cycle fatigue (LCF) testing is utilized to assess the candidate alloys' intrinsic fatigue capabilities. In addition, a low coefficient of thermal expansion (CTE) is desirable since the CTE largely controls, for a given thermal cycle, the magnitude of the thermally induced strains. The primary aim of this study was to compare the LCF performance of recently developed low CTE, high strength HAYNES® 244® alloy to that of Waspaloy, a legacy case alloy, from room temperature to 1400 °F (760 °C). A secondary aim was to shed light on the active deformation and damage mechanisms in these alloys. We observed that both alloys exhibited comparable fatigue lives, within experimental scatter, but the 244 alloy deformed by deformation twinning, whereas Waspaloy deformed by dislocation slip and precipitate shearing and looping.

**B-6: Microstructure and Mechanical Properties of a Novel  $\gamma'$ -strengthened Multi-component CoNi-based Wrought Superalloy:** *Li Huiwei*<sup>1</sup>; Zhang Xiaorui<sup>2</sup>; Lu Song<sup>2</sup>; Zhuang Xiaoli<sup>2</sup>; Li Longfei<sup>2</sup>; Wen Xinli<sup>1</sup>; Feng Qiang<sup>2</sup>; <sup>1</sup>Beijing Beiyue Functional Materials Corporation; <sup>2</sup>University of Science and Technology Beijing

To reveal the deformation behavior of a novel  $\alpha$ -strengthened multi-component CoNi-based wrought superalloy, the tensile properties from room temperature to 850 °C and creep property under 725 °C/630 MPa were studied. The results show that after hot forging and sub-solvus solution plus two-step aging heat treatment, the grain size of the investigated alloy is uniform, accompanied by the bimodal distribution of  $\alpha$  precipitates. Elements such as Co, Cr, and Mo segregate within the  $\alpha$  phase, whereas Al, W, Ni, Ti, and Ta exhibited segregation in the  $\alpha$  precipitate. In comparison with typical wrought superalloys U720Li and Waspaloy, the investigated alloy exhibits enhanced yield strength at 750 ~850 °C, which may be associated with the alloy's larger grain size and the increase in the intermediate temperature flow stress anomaly inherent to Co-based alloys. Meanwhile, the creep property of the investigated alloy surpasses those of alloys U720Li and Waspaloy, which is primarily attributed to its larger grain size and relatively higher  $\alpha'$  volume fraction. Additionally, the lower stacking fault energy of the alloy facilitates the formation of stacking faults and micro-twins, further enhancing its creep property. The findings of this study will hold importance for the further optimization of CoNi-based wrought superalloys.



**B-7: Stress-induced Acceleration of the Growth of  $\delta$ -Phase Precipitates in Ni-based Superalloy GH4169 (IN718) and Its Effect on Acceleration of Intergranular Cracking Under Creep Loading at Elevated Temperature:** *Ayumi Nakayama*<sup>1</sup>; Run-Zi Wang<sup>1</sup>; Ken Suzuki<sup>1</sup>; Hideo Miura<sup>1</sup>; <sup>1</sup>Tohoku University

In this study, intermittent creep tests and EBSD (Electron Backscatter diffraction) analyses were conducted on GH4169 (IN718) at 800°C to elucidate the change mechanism of its micro texture and the degradation mechanism of the strength of grain boundaries under mechanical loading at elevated temperature. Under creep loading, the growth of  $\delta$ -phase (Ni<sub>3</sub>Nb) precipitates was found to be accelerated around grain boundaries. This growth of  $\delta$ -phase precipitates caused the disappearance of the solute strengthened phase in the surrounded grains and, thus, the effective strength of grains decreased. Even though the precipitation around grain boundaries increased their effective strength at first, however, it started to decrease with time due to the acceleration of the growth and accumulation of vacancies and dislocations around the interface between the precipitates and the matrix. This acceleration was attributed to the large lattice mismatch between the precipitate and the matrix, and the structural singularity around the edges of the needle-shape precipitates. Finally, intergranular cracking was accelerated. The degradation of the strength of the material was validated by using a micro tensile test using a scanning electron microscope. The acceleration process was successfully explained by the concept of the stress-induced acceleration of diffusion, by applying the modified Arrhenius equation. The growth time of  $\delta$ -phase precipitates around grain boundaries was also predicted quantitatively.

**B-8: The Effect of Direct Current Heating on the Creep Behaviour of Polycrystalline Ni-based Superalloys:** *Ryo Sasaki*<sup>1</sup>; Satoshi Utada<sup>2</sup>; Yuanbo Tang<sup>2</sup>; Carlos Nunes<sup>3</sup>; Roger Reed<sup>2</sup>; <sup>1</sup>Proterial; <sup>2</sup>University of Oxford; <sup>3</sup>University of São Paulo

This study discusses the effect of the direct current heating (DCH) on the creep behaviour of Ni-based superalloys, in an attempt to converge on best practice and also reliability. Particular features are the use of an electro-thermal mechanical testing (ETMT) system which has allowed for direct comparison of the DCH heating method with the more conventional resistance furnace heating (FH) approach. In addition, particular attention is paid to a testing protocol to confirm the accuracy of temperature measurement during DCH. Waspaloy, Alloy713C and Alloy246 are used in different geometrical configurations, thus enabling us to establish the difference in creep behaviours caused by altering the sample sizes and the heating methods. The creep rupture lives of the materials tested by the DCH method were consistently shorter than that tested by the FH method. Microstructural investigation revealed that there is no influence of heating method on the coarsening rate of the fine precipitates and on the thickness of the oxide layer in Waspaloy during creep test at 732 °C. Moreover, the presence of an axial temperature gradient did not influence the creep life unduly. The radial temperature gradient as estimated by an analytical model has affected to some extent. It is hypothesised that the diffusivity is increased by the direct current, and the dislocation climb is facilitated in the DCH testing for Waspaloy.

**B-9: The PLC Effect in the Absence of Long-range Cottrell Atmospheres in RR1000:** *Bradley Rowlands*<sup>1</sup>; James Miller<sup>1</sup>; Lewis Owen<sup>2</sup>; Howard Stone<sup>1</sup>; Wenwen Song<sup>3</sup>; Xiao Shen<sup>3</sup>; Enrique Galindo-Nava<sup>4</sup>; Cathie Rae<sup>1</sup>; <sup>1</sup>University of Cambridge; <sup>2</sup>University of Sheffield; <sup>3</sup>RWTH Aachen University; <sup>4</sup>University College London

The Portevin-Le Chatelier (PLC) effect is widely attributed to the partitioning of interstitial C atoms around dislocation cores in mild steels, to form Cottrell atmospheres. However, limited empirical evidence exists to clarify how similar mechanisms extend to complex multicomponent alloy systems such as Ni-based superalloys. The presence of the PLC effect was demonstrated in coarse-grained RR1000 from 200 °C – 550 °C through digital image correlation (DIC). The effect was also demonstrated in simple binary Ni-(20-25) Cr (wt. %) alloys, suggesting that the microstructural complexity of superalloys is not key to elucidating the atomistic origins. Probe-corrected scanning transmission electron microscopy (STEM)-energy dispersive X-ray spectroscopy and atom probe tomography were performed on interrupted specimens displaying the PLC effect. No evidence of long-range solute enrichment was observed in the vicinity of dislocation cores. Hence, alternative origins for the effect were considered; evidence for short-range order was assessed in Ni-Cr powder through neutron diffraction. A preference was observed for particular local configurations of Ni and Cr atoms within a unit cell, resembling, but not identical to, those in long-range ordered Ni<sub>2</sub>Cr. High resolution STEM imaging demonstrated the presence of nanodomains in Ni-Cr and RR1000 containing diffraction contrast effects resembling superlattice fringes. STEM image simulations based on refined unit cell structures demonstrated that such features may relate to the local lattice distortion in short-range ordered (SRO) domains. The results do not support the presence of long-range Cottrell atmospheres within the temperature range of the PLC effect, but instead of SRO, an alternate hypothesised origin of the PLC effect.

**B-10: Microstructure-based Modeling of Temperature-dependent Yield Strength in Polycrystalline Ni-base Superalloys:** *Moritz Müller*<sup>1</sup>; Howard Stone<sup>2</sup>; Enrique Galindo-Nava<sup>3</sup>; Felix Schleifer<sup>1</sup>; Michael Fleck<sup>4</sup>; Uwe Glatzel<sup>1</sup>; <sup>1</sup>University of Bayreuth; <sup>2</sup>University of Cambridge; <sup>3</sup>University of College London

A new model for the temperature-dependent yield strength of polycrystalline Ni-base superalloys at high strain rates ( $10^{-3}$  to  $10^{-4}$ s<sup>-1</sup>) featuring multimodal precipitate microstructures is presented. It extends existing mean field models based on the summation of particle strengthening and other strengthening contributions, which were originally created to describe behavior at room temperature. Temperature dependence is introduced for each contribution using existing models or datasets from the literature while maintaining physical validity and avoiding unnecessary fitting parameters. Further, the expected change in the precipitate distributions at high temperatures is achieved using CALPHAD. By considering such microstructural changes, the model can predict the yield strength from room temperature to beyond the solvus temperature of the precipitates. Due to the strategy for combining different strengthening contributions, the model can also predict the active deformation modes at any temperature and can be extended easily to incorporate additional deformation mechanisms. The model's sensitivity to microstructural parameters and its strengths and weaknesses are also discussed. Application of the model to three commercial alloys shows good agreement over the whole temperature range.

---

## General Session 4: Disk Alloy Mechanical Behavior II

Monday PM | September 9, 2024  
Exhibit Hall | Seven Springs Mountain Resort

**Session Chair:** Howard Stone, University of Cambridge; Michael G. Fahrman, Haynes International

---

**8:10 PM**

### High Temperature Crack Growth Characteristics Under Dwell-fatigue in a PM Superalloy for Disc Applications: *Hangyue Li*<sup>1</sup>;

<sup>1</sup>University of Birmingham

Crack growth characteristics under dwell-fatigue loading are investigated in this paper for a new PM nickel superalloy developed by Rolls-Royce plc. In order to achieve a good balance of mechanical properties, it is critical that an appropriate heat treatment be defined for the alloy. Here, the influences of cooling rate after solution heat treatment on  $\gamma'$  size and distribution, grain boundary serration and dwell-fatigue crack growth resistance are first investigated. A medium cooling rate has been found to produce good dwell-fatigue crack growth resistance and has been carried forward to a comprehensive matrix of dwell-fatigue growth testing in air with varied temperatures (700 and 760 C), initial K values, and testing procedures (constant amplitude loading and load shedding). Tests have also been interrupted to allow detailed examination of crack tips using scanning electron microscopy. Notably the dwell time is 120 s (positioned at maximum load), and the applied stress ratio is fixed at 0.1. Significant variations in behaviour are observed at both temperatures. It is concluded that the variation in crack growth rates results from the selection and interactions between two different time-dependent mechanisms: environmentally assisted oxide forming and cracking, and environmental independent creep deformation and creep crack growth. When the environmentally related mechanism operates alone, the fastest crack growth rates are obtained. This study demonstrates that the environmentally assisted, sustained fast crack growth can be inhibited with a combination of an appropriate microstructure and a defined range of mechanical driving force.

**8:35 PM**

### Strain Rate Effect on Strain Localization in Alloy 718 Ni-based Superalloy at Intermediate Temperature: *Malo Jullien*<sup>1</sup>; Rephayah Black<sup>2</sup>; Marc Legros<sup>3</sup>; Jean-Charles Stinville<sup>2</sup>; Damien Texier<sup>1</sup>; <sup>1</sup>Institut Clement Ader; <sup>2</sup>University of Illinois Urbana-Champaign; <sup>3</sup>CEMES

Tensile tests on Alloy 718 Ni-based superalloy at 650 °C at different strain rates revealed a strain-rate dependency on the fracture mode. A change from intergranular to transgranular fracture was observed in air as the strain rate increased, mainly when Portevin-Le-Chatelier (PLC) mesoscopic deformation bands were present. To better understand the link between strain rate and fracture mode, a description of the strain localization in the early deformation stage is needed. In this study, high-resolution digital image correlation (HR-DIC) was carried out at the onset of strain localization at low strain rate (LSR,  $\dot{\epsilon} = 10^{-4} \text{ s}^{-1}$ ) and at high strain rate (HSR,  $\dot{\epsilon} = 10^{-2} \text{ s}^{-1}$ ), this latter condition aimed at investigating the microplasticity development within PLC bands. The in-plane and out-of-plane displacement components of each single plastic event were measured to accurately assess and distinguish morphological sliding at grain boundaries (i.e., grain boundary sliding) and dislocation slip. The deformation within the PLC bands was examined at macro, meso, and microscales. Statistical analyses highlighted the distribution and partitioning of these strain localization events related to different microstructural features, including grains, and grain and twin boundaries. Grain boundary sliding was found to be more prominent at LSR. Interestingly, events near and parallel to twin boundaries are particularly intense regardless of the strain rate. At HSR, grain boundary sliding is less pronounced, and a high density of intragranular slip bands developed within the PLC bands based on observations before and after the occurrence of the PLC band.

**9:00 PM**

### Influence of Pre-spinning Induced Plastic Strain on Microstructures and Mechanical Properties of Superalloy Disc Forgings: *Wenyun Zhang*<sup>1</sup>; *Shifu Chen*<sup>1</sup>; *Shanjie Yang*<sup>1</sup>; *Linhan Li*<sup>1</sup>; *Beijiang Zhang*<sup>1</sup>; <sup>1</sup>China Iron & Steel Research Inst Group

Residual stress is one of the major factors that reduces the dimension stability of superalloy disc components during either machining or in service. A pre-spinning operation has been proved to be an effective technique to modify the unfavorable residual stress in disc forgings. By spinning the semi-finished disc forgings up to a certain rotational speed, a small amount of plastic strain is generated and accordingly results in a redistribution of the internal stress. The spinning generated plastic strain, though quite small, significantly affects the mechanical properties of the disc forgings. To ensure the efficiency and reliability of the application, a clear understanding of the effects of the pre-spinning generated plastic strain needs to be obtained. The two widely employed disc alloys GH4065A and FGH4096 were evaluated using a specifically designed, full-scale spinning experiment, the microstructure and the mechanical properties prior to and after the spinning were analyzed in detail. The results show that the pre-spinning generated a higher dislocation density which is heterogeneously distributed. The dislocations tend to accumulate at the various types of internal interfaces and within primary precipitates. The formation of heterogeneous dislocation structures significantly affects the mechanical properties, including, but not limited to, the tensile strength, creep, and fatigue crack growth behavior. By optimizing the spinning parameters, the mechanical properties can be well controlled to meet the design requirements for disc forgings.

## General Session 5: Blade Alloy Mechanical Behavior

Tuesday AM | September 10, 2024  
Exhibit Hall | Seven Springs Mountain Resort

**Session Chair:** Caspar Schwalbe, MTU Aero Engines AG

### 8:30 AM

**Tensile Testing of Ni-based Single Crystal Superalloys: What is the Correct "Point of View"?:** Satoshi Utada<sup>1</sup>; Qinan Han<sup>2</sup>; Ang Li<sup>2</sup>; Melvin Miquel<sup>1</sup>; Celal Polatolu<sup>1</sup>; Magnus Hasselqvist<sup>3</sup>; Yuanbo Tang<sup>1</sup>; Roger Reed<sup>1</sup>; <sup>1</sup>University of Oxford; <sup>2</sup>Nanjing University of Aeronautics and Astronautics; <sup>3</sup>Siemens Energy AB

The anisotropy of deformation of a single crystal superalloy is studied using a newly designed furnace arrangement which allows for videography from multiple apertures and subsequent digital image correlation (DIC). Thus, for initially cylindrical specimens, the full field of surface strain is measured at a 25  $\mu$ m spatial resolution. Our approach is tested for STAL15 along each of the  $\langle 001 \rangle$ ,  $\langle 011 \rangle$ , and  $\langle 111 \rangle$  crystallographic orientations at 800 °C. The time-dependent anisotropic deformation along each of these crystallographic directions is quantified. Crystal plasticity finite element (CPFE) calculations are used to rationalise the observations; it is demonstrated that the predictions are particularly sensitive – on account of the plastic anisotropies – to the boundary conditions used for the loading. Implications for the testing of single crystal superalloys are discussed in detail, with a particular view towards improving testing protocols.

### 8:55 AM

**Mechanisms of Dwell Fatigue in Single Crystal Ni-base Superalloys at Intermediate Temperatures:** Jane Woolrich<sup>1</sup>; Simon Gray<sup>2</sup>; Ian Edmonds<sup>1</sup>; Edward Saunders<sup>1</sup>; Catherine Rae<sup>3</sup>; <sup>1</sup>Rolls-Royce plc; <sup>2</sup>Cranfield University; <sup>3</sup>University of Cambridge

Single crystal (SX) nickel-base superalloys have been developed specifically to withstand the high temperatures that would engender severe creep degradation in a lesser alloy. Use in gas turbine blades has long been a driver for the development of ever more capable alloys that can survive higher temperatures without significant material damage[1]. The drive for increased financial efficiency has included a desire for increased duration, and longer time between overhauls, as well as reduced specific fuel consumption. The long-term behaviour of SX alloys at lower temperatures, such as that experienced at the blade root fixings, has not historically influenced alloy design, but has become increasingly important as the target time between overhauls increases. This study looks at the behaviour of an example of a 2nd, 3rd and 4th generation SX alloy at a temperature commensurate with that outside the gas path, in keeping with that around the blade root. The influence of dwell on both the predicted life and consequent fractography is examined. In addition, the dependence of crack growth rate with secondary orientation is assessed. Finally, the crack trajectory close to the crack tip is considered and the possible influence of different regions of the loading cycle discussed.

### 9:20 AM

**Anisotropic Tensile Properties of Ni-based Single-crystal Superalloys: A Phase-Field-Informed Crystal-plasticity Finite-element Investigation:** Jean-Briac Le Graverend<sup>1</sup>; Rajendran Hari Krishnan<sup>1</sup>; <sup>1</sup>Texas A&M University

Ni-based single-crystal superalloys, mostly used in turbine blade applications, are inherently anisotropic and usually cast in the  $\langle 100 \rangle$  direction. Any slight misorientations result in anomalies in the microstructural evolution, thereby, causing variation in the mechanical response. As the stability of the microstructure dictates the structural integrity of the blade, it is essential to understand the microstructural state as a function of the crystallographic orientation. Therefore, to predict the microstructural evolution of single-crystal superalloys at any given orientation on the standard stereographic triangle, a crystallographic-sensitive phase-field model was developed. The phase-field simulations for the perfect  $\langle 100 \rangle$ ,  $\langle 011 \rangle$ , and  $\langle 111 \rangle$  orientations agreed well with the experimental characterizations. For the first time, a model also predicts the microstructures for misorientations ( $10^\circ$ ) away from the main crystallographic directions. Finally, for a quantitative assessment of the macroscale performance of various orientations, the 3D phase-field microstructures were employed to carry out crystal-plasticity finite-element (CPFE) micromechanical simulations for strain-controlled monotonic tensile tests at 1050 °C.

### 9:45 AM

**Retardation and Acceleration of Dwell-fatigue Crack Propagation in Ni-base Superalloys: Experimental and Numerical Investigations on CMSX-4 and IN718:** Shiyu Suzuki<sup>1</sup>; Hayato Matsuoka<sup>2</sup>; Qihe Zhang<sup>2</sup>; Zhiqi Chen<sup>2</sup>; Itsuki Sasakura<sup>2</sup>; Motoki Sakaguchi<sup>2</sup>; <sup>1</sup>Japan Aerospace Exploration Agency; <sup>2</sup>Tokyo Institute of Technology

Effect of tensile dwell on crack propagation under subsequent fatigue loading during dwell-fatigue crack propagation in Ni-base superalloys was investigated using a single crystal superalloy, CMSX-4, and a wrought superalloy, IN718. Crack propagation tests with single tensile dwell introduced during pure fatigue loading under various conditions of stress intensity and dwell time were conducted at 900 °C and 650 °C for CMSX-4 and IN718, respectively. In CMSX-4, fatigue crack retardation occurred after the tensile dwell, which was attributed to stress relaxation induced by creep deformation during the dwell and the resultant residual compressive stress during the subsequent fatigue loading. Fatigue crack propagation rate after the tensile dwell was quantified by evaluating effective stress intensity factors based on the residual compressive stress field obtained by finite element analysis. In IN718, acceleration of the fatigue crack propagation occurred after the tensile dwell at high  $K_{max}$  values whereas the retardation occurred following temporary acceleration after the dwell at low  $K_{max}$  values. The acceleration was attributed to grain boundary (GB) damage caused by oxygen diffusion along the GBs induced by high stress near the crack tip during the tensile dwell. The transition from the crack retardation to the acceleration in IN718 was rationally explained based on a size relationship between the stress relaxation area and the GB damage zone around the crack tip caused by the tensile dwell.

## Interactive Session C: Blade Alloy Processing & Mechanical Behavior

Tuesday AM | September 10, 2024  
Winterberry | Seven Springs Mountain Resort

**C-1: Effect of Re Addition on the Sensitivity to Recrystallization in As-cast Ni-based SX Superalloys:** *Yihang Li<sup>1</sup>; Zhipeng Jiang<sup>1</sup>; Longfei Li<sup>2</sup>; Guang Xie<sup>2</sup>; Jian Zhang<sup>2</sup>; Qiang Feng<sup>1</sup>*; <sup>1</sup>University of Science and Technology Beijing; <sup>2</sup>Institute of Metal Research, Chinese Academy of Sciences

The recrystallization of nickel-based single-crystal superalloys during solution treatment may be promoted by local deformation induced during the cooling stage of directional solidification and is related to alloy chemistry. In this study, the effect of Re addition on the sensitivity to recrystallization of nickel-based single-crystal superalloys and the ways in which Re affects nucleation and growth of recrystallized grains are investigated using the as-cast alloy without Re addition and those with Re addition of 2 and 4 wt.%. It is suggested that 4 wt.% Re addition can significantly increase the propensity to nucleate recrystallized grains but significantly inhibit grain growth of the as-cast SX superalloy. The former is attributed to the increase of Re segregation at the dendrite scale, which leads to the increase of strength difference in  $\bar{a}$  matrix of the dendrite core and interdendritic region, as well as the increase in eutectics and casting pores, thus providing higher stored energy and more nucleation sites for recrystallization nucleation. Meanwhile, the severe Re segregation in  $\bar{a}$  matrix of high-Re alloys increases the  $\bar{a}$  solvus temperature and reduces the precipitate-free zone, thus inhibits growth of recrystallized grains. These insights will be beneficial to alloy design and process optimization and allow further improvement of the casting costs.

**C-2: Effects of Trace Impurities in Ni-base Single Crystal Superalloys on High-temperature Properties and Disablement of Impurities by CaO for Recycle of Superalloys:** *Kyoko Kawagishi<sup>1</sup>; Chihiro Tabata<sup>2</sup>; Tadaharu Yokokawa<sup>1</sup>; Yuji Takata<sup>1</sup>; Michinari Yuyama<sup>2</sup>; Takahide Horie<sup>2</sup>; Hirotochi Maezawa<sup>2</sup>; Shinsuke Suzuki<sup>2</sup>; Hiroshi Harada<sup>1</sup>*; <sup>1</sup>National Institute for Materials Science; <sup>2</sup>Waseda University

In determining the specifications for the production or recycling process of Ni-base single crystal superalloys, it is important to clarify the allowable trace impurity concentration. In this study, the effects of Pb and Sb on high-temperature strength and oxidation resistance of 6th generation superalloy TMS-238 were summarized. It was found that both Sb and Pb do not have a large effect on creep rupture life, but they degrade oxidation resistance. The removal of impurities by melting in a CaO crucible was tested and its mechanism was examined. It was found that Ca forms a compound with impurities within the alloy and prevents the segregation of impurities at the oxide film/substrate interface. The effect of CaO was also confirmed in an experiment in which impurity S was removed from 1st generation Ni-base superalloy TMS-1700 by adding CaO particles in a 3-ton commercial melting furnace. Similar results were obtained for this alloy, where it was also found that CaS had formed inside the alloy, thus improving the oxidation resistance of TMS-1700.

**C-3: On the Effect of Super-solidus Heat Treatments on the Microstructure and Creep Properties of a Third-generation Single Crystal Ni-based Superalloy:** *Inmaculada López Galilea<sup>1</sup>; Lisa Hecker<sup>1</sup>; Marc Sirrenberg<sup>1</sup>; Sebastian Weber<sup>1</sup>*; <sup>1</sup>Ruhr University Bochum

A Super-Solidus Hot Isostatic Pressing, SSHIP, heat treatment has been developed and applied to the third-generation Ni-based single crystal superalloy CMSX-4 Plus. The aim of this new type of heat treatment is to significantly reduce the solution heat treatment time and improve the mechanical properties compared to those resulting from subjecting the single crystal to conventional heat treatment routes. The partial melting of the regions with the lowest solidus temperatures during SSHIP results in the acceleration of the diffusional processes, while the control of the cooling rate after SSHIP results in the optimum precipitation of the fine  $\gamma/\gamma'$  microstructure. This innovative type of heat treatment, which can significantly reduce the economic penalties associated with lengthy high-temperature solution treatments while having a positive effect on the final mechanical properties, could be applied to other complex single crystal Ni-based superalloys containing large amounts of refractory elements (like rhenium, tungsten, and tantalum), showing strong dendritic segregation and / or a large volume fraction of eutectics in the as-cast state.

**C-4: Exploring Microstructural Characteristics, Mechanical Behavior, Hydrogen Embrittlement and Long-term Stability of Polycrystalline CoNiCr-based Superalloys:** *Svetoslava Tsankova<sup>1</sup>; Oliver Nagel<sup>1</sup>; Andreas Bezold<sup>1</sup>; Bianca Grandjean<sup>1</sup>; Andreas Kirchmayer<sup>1</sup>; Mathias Göken<sup>1</sup>; Steffen Neumeier<sup>1</sup>*; <sup>1</sup>Friedrich-Alexander-Universität Erlangen-Nürnberg

Polycrystalline  $\gamma/\gamma'$ CoNiCr-based superalloys have a promising combination of properties for aerospace and stationary gas turbine applications. In this study, four alloys, CoWAlloy1, 2, 3 and 6, were selected for further investigation. Microstructures of fully heat-treated materials were characterized by scanning and transmission electron microscopy and long-term stability at 750 °C was examined for various durations up to 1000 h. Tensile tests were performed between 25 °C and 700 °C, revealing dynamic strain aging in CoWAlloy2, 3 and 6 at intermediate temperatures of 400-650 °C. Hydrogen charging induced a decrease in tensile ductility at 25°C in the  $\mu$  phase containing CoWAlloy3. Creep experiments were performed on CoWAlloy1, an alloy with increased Ti and Ta content, at 750 °C and 800 MPa, with variations of the secondary  $\gamma'$  precipitate size and grain size to identify optimal microstructural parameters. It was found that smaller grain sizes lead to a significantly higher creep resistance at these testing conditions.

### C-5: Revisiting Nanoscale Microstructural Features of Alloy 680 to Understand its Remarkable Mechanical Strength in the As-welded

**Condition:** Cleiton Silva<sup>1</sup>; Rafaella Silva<sup>1</sup>; Emerson Miná<sup>1</sup>; Ricardo Reppold<sup>2</sup>; Marcelo Paes<sup>2</sup>; Giovanni Dalpiaz<sup>2</sup>; Marcelo Motta<sup>4</sup>; Hélio de Miranda<sup>1</sup>; Irina Wossack<sup>3</sup>; Alisson Kwiatkowski da Silva<sup>3</sup>; Christian Liebscher<sup>3</sup>; <sup>1</sup>Universidade Federal do Ceará; <sup>2</sup>Petróleo Brasileiro S/A; <sup>3</sup>Max-Planck-Institut für Eisenforschung GmbH

The present study assesses the microstructure of a new Ni-based alloy filler metal, Inconel® 680, at high resolution to understand the underlying mechanisms behind its remarkable mechanical properties. Investigations using aberration-corrected (scanning) transmission electron microscopy (TEM/STEM) were performed to complement the previous microstructural analysis. The results from TEM analysis confirmed Nb-rich C14-type Laves phase precipitation, besides different types of carbides in the interdendritic spacings. However, the advanced microstructural characterisation has also shown a heterogeneous pattern in terms of microstructure between the cellular-dendrite core and interdendritic region. A higher dislocation density was noticed in the interdendritic spacings accompanied by nanometric precipitation. These nanoprecipitates were identified as being tined globular-shape -Ni<sub>3</sub>Nb phase. The -Ni<sub>3</sub>Nb phase precipitation resulted from an intense microsegregation of Nb during the solidification. This precipitation of the -Ni<sub>3</sub>Nb phase plays an essential role in the enhanced yield strength of alloy 680.

### C-6: Creep Properties Dependence to Solution Heat Treatment of Second and Third Generation Ni-based Single Crystal Superalloys:

Luciana Maria Bortoluci Ormastroni<sup>1</sup>; Jeremy Rame<sup>2</sup>; Jonathan Cormier<sup>3</sup>; <sup>1</sup>Safran Aircraft Engines; <sup>2</sup>NAAREA; <sup>3</sup>Institut Pprime/ENSMA

Computational design is increasingly being used by industry and research institutes for the development of new compositions of Ni-based single crystal (SX) superalloys. Alloy selection is often based on the mechanical properties of the fully heat-treated Ni-based SX superalloys. However, a more complex chemical composition leads to a more complex solution heat treatment (ST). The development of a ST to reach optimum homogenization, requires time and resources, overall penalizing the time/cost savings provided by computational design approaches. Thus, the present study investigates several superalloys "as cast" mechanical properties to predict the creep life of the solution heat treated alloy. Four commercial superalloys with distinct chemical composition were chosen. Each alloy was investigated in (i) the as cast (AC) and (ii) solution treated and aged (ST) states. The superalloys were creep tested at 950 °C/390 MPa and 1050 °C/190 MPa. A creep life improvement by a factor of 1.5 to 3 times has been observed after the ST, irrespective of the alloy chemical composition or creep test conditions. Down-selecting alloys' composition from the as-cast creep properties can be a viable approach to speed-up alloy design.

### C-7: Option of HIP Implementation Scheme and its Effects on the Mechanical Properties of a Nickel-based Single-crystal Superalloy:

Siliang He<sup>1</sup>; Longfei Li<sup>1</sup>; Song Lu<sup>1</sup>; Yunsong Zhao<sup>2</sup>; Jian Zhang<sup>2</sup>; Qiang Feng<sup>1</sup>; <sup>1</sup>University of Science and Technology Beijing; <sup>2</sup>Science and Technology on Advanced High Temperature Structural Materials Laboratory Beijing Institute of Aeronautical Materials

The micropores and residual eutectic in nickel-based single crystal (SX) superalloys can promote crack initiation in the SX turbine blades during service, threatening the components safety. Hot isostatic pressing (HIP) treatment is an effective technique to reduce micropores and enhance the mechanical properties of the alloys. This work investigated the effect of two typical HIP implementation schemes on a nickel-based SX superalloy compared with a conventional heat treatment scheme (without HIP). The results show that the HIP-treated samples had fewer micropores, residual eutectic and better mechanical properties than that of the non-HIP sample. The HIP treatment can increase the yield strength, elongation and reduction in area of tensile properties at 760 °C compared with the non-HIP sample, but had no noticeable effect on that at 980 °C. The HIP treatment on the solution-treated sample enhanced the creep rupture life more than that of the as-cast sample at 980 °C/ 250 MPa, but had no influence on it at 1100 °C/ 130 MPa. The HIP effect on the fatigue rupture cycles was closely related to the type of crack initiation site. The HIP treatment significantly prolonged the rupture cycles of low-cycle fatigue (LCF) at 760 °C and high-cycle fatigue (HCF) at 850 °C of HIP-treated samples by changing the crack initiation sites, but had no impact on that at 980 °C. Comparing different HIP implementation schemes on microstructures and comprehensive mechanical properties, the HIP treatment on the solution-treated sample was better than that on the as-cast sample. This work can improve the mechanical properties and provide guidance for HIP implementation scheme of nickel-based SX superalloys.

### C-8: Tensile Behavior of TMS-238 Ni-based Single-crystal Superalloy at 650°C:

Benoît Mansoz<sup>1</sup>; Pierre Caron<sup>2</sup>; Kyoko Kawagishi<sup>3</sup>; Luciana Maria Bortoluci Ormastroni<sup>4</sup>; Patrick Villechaise<sup>5</sup>; Jonathan Cormier<sup>5</sup>; Florence Pettinari-Sturmel<sup>1</sup>; <sup>1</sup>CEMES - CNRS, University of Toulouse; <sup>2</sup>Scientific Consultant; <sup>3</sup>National Institute for Materials Science (NIMS); <sup>4</sup>Safran Aircraft Engines; <sup>5</sup>Institut PPrime, ISAE-ENSMA

TMS-238 is a promising 6th generation superalloy with impressive high temperature creep performance but it exhibits a particular tensile behavior at 650 °C with low yield strength, limited ductility and a non-classical hardening behavior. To study this behavior, TMS-238 specimens with different misorientations away from the perfect [001] crystallographic orientation were tensile tested at 650 °C. Mechanical tests revealed that highly misoriented specimens do not exhibit this atypical hardening behavior but a classical "plateau" behavior and keep a similar low yield strength. TEM investigations were conducted with *post mortem* observations in order to interpret these macroscopic tensile characteristics. Similar TEM experiments were also performed using other more classical alloys for reference. TEM investigations in TMS-238 revealed a high density of dislocations and stacking faults in the  $\gamma$  phase and a homogeneous deformation in the perfect [001] oriented samples, contrarily to the heterogeneous deformation observed in the misoriented specimen. TEM energy disperse X-ray spectroscopy analysis confirmed significant amounts of Re and Ru in  $\gamma$ , two elements known to increase the  $\gamma/\gamma'$  misfit and decrease fault energy, resulting in a lower mobility of dislocations in the matrix, the presence of extended stacking faults in the vertical  $\gamma$  - channels and a strong hardening.

**C-9: In Situ Imaging of Misorientation Changes During Tensile Loading in Single Crystal Nickel-base Superalloys by High-resolution X-ray Diffraction Mapping:** *Robert Albrecht*<sup>1</sup>; <sup>1</sup>University of Silesia

Recently, the method called high-resolution imaging of misorientations in single crystals has demonstrated its usefulness in accurately determining the single crystal quality in superalloys. This was made possible by obtaining high-resolution angular measurements of misorientation (arc-sec) and high-resolution imaging ( $\mu\text{m}$ ) combined with a relatively large measurement area. The technique combines traditional X-ray diffraction topography with high-resolution diffraction and advanced data post-processing, including color coding and 3D projections of diffraction images. It was demonstrated that the mosaic structure of superalloys is highly complex and varies at both the micro and macro levels. In the present work, the advanced high-resolution X-ray diffraction method for imaging misorientation and mosaicity in single crystal superalloys was used to observe structural changes during uniaxial tensile loading. This research utilized single crystal flat tension samples from CMSX-4 superalloy prepared from the casting produced at a 3 mm/min withdrawal rate. The results indicate that the crystallographic orientation changes are within a few degrees up to the rupture. The evolution of the plastic deformation region was directly observed on the samples by contrast blurring.

**C-10: A Prediction Method for Local Creep Strain of Directionally Solidified Superalloys and Turbine Blades:** *Song Lu*<sup>1</sup>; *Yikai Shao*<sup>1</sup>; *Weiwei Zheng*<sup>1</sup>; *Longfei Li*<sup>1</sup>; *Qiang Feng*<sup>1</sup>; <sup>1</sup>University of Science and Technology Beijing

Evaluating the service conditions and the corresponding strain at high-pressure turbine blades is crucial for the safe service and maintenance of aircraft engines. However, due to the harsh environment in turbines and the complex geometry of blades, it is difficult to directly monitor the variation of their service temperatures, stresses and strains. In this work, an approach to predicting the equivalent service conditions and the local strain of directionally solidified superalloys and turbine blades was developed by integrating high-throughput creep tests and machine-learning tools. A large amount of experimental data was obtained using the flat specimens with the continuously variable cross-section and digital image correlation technique. Then, the quantitative relationship between temperature, stress, strain, time and the essential microstructure parameters was established under the help of machine learning models. The established machine learning models were then employed to predict the service conditions and the corresponding strain of a directionally solidified superalloy and a turbine blade. Finally, the applicability and limitations of this method were discussed. The development of this method provides guidance for the service evaluation of turbine blades.

**C-11: Prediction of the Creep Strength of Single Crystalline Superalloys via a Microstructure-informed Deep Neural Network:** *Andreas Bezold*<sup>1</sup>; *Toni Albert*<sup>1</sup>; *Mathias Göken*<sup>1</sup>; *Steffen Neumeier*<sup>1</sup>; <sup>1</sup>Friedrich-Alexander-Universität Erlangen-Nürnberg

The design of superalloys is traditionally based on numerous experimental iterations guided by expert insights. The advent of computational tools that can calculate and predict thermophysical and mechanical properties has transformed this process. These tools have facilitated the discovery and evaluation of new alloys, leading to advancements in high-temperature capabilities and other design objectives, such as reducing the content of Re.

**C-12: Temperature and Time Dependence of Elemental Segregation at Stacking Faults in Ni- and Co-base Superalloys:** *Nicolas Karpstein*<sup>1</sup>; *Mingjian Wu*<sup>1</sup>; *Andreas Bezold*<sup>1</sup>; *Steffen Neumeier*<sup>1</sup>; *Jonathan Cormier*<sup>2</sup>; *Erdmann Spiecker*<sup>1</sup>; <sup>1</sup>FAU Erlangen-Nürnberg; <sup>2</sup>Institut Pprime, ISAE-ENSMA

Elemental segregation at stacking faults in the  $\gamma'$  phase is a crucial part of the stacking-fault based deformation of superalloys, and the local composition of a stacking fault critically affects the resistance of  $\gamma'$  to further shearing. Here, the process of elemental segregation at extrinsic stacking faults in  $\gamma'$  is examined in Ni-base superalloy CMSX-4 and Co-base superalloy ERBOCo-4. By measuring fault compositions not only after deformation, but also after additional load-free annealing steps of different durations and temperatures between 700 °C and 900 °C, time- and temperature-dependent aspects of the segregation process are revealed. It is shown that elemental segregation continues to evolve toward an equilibrium composition after a fault has formed, indicating that fully formed stacking faults still provide a driving force for segregation processes and that their equilibrium composition can differ from that which they obtain during their formation. As the elemental segregation process is diffusion-based, it is observed to be considerably slower at a lower temperature. In both alloys, the segregation trends observed after annealing depend on the annealing temperature: A lower temperature promotes a more  $\gamma'$ -like fault composition associated with  $\gamma'$  softening; conversely, at higher temperatures, the fault composition tends toward that of the  $\eta$  phase, which is considered beneficial in the context of local phase transformation strengthening. As  $\eta$ -like segregation also involves the enrichment of slowly diffusing tungsten, kinetics likely play a role in the observed temperature dependence.

---

## General Session 6: Blade Alloy Processing

Tuesday AM | September 10, 2024  
Exhibit Hall | Seven Springs Mountain Resort

**Session Chairs:** Roger Reed, University of Oxford; Corey O'Connell, Special Metals

---

### 11:20 AM

**Resistance to Viscoplastic Deformation of Ni-based SX Superalloys with Bimodal Distributions of Gamma-prime Precipitates:** *Luciana Maria Bortoluci Ormastroni*<sup>1</sup>; Jeremy Rame<sup>2</sup>; Dominique Eyidi<sup>3</sup>; Fabio Machado Alves da Fonseca<sup>4</sup>; Jonathan Cormier<sup>5</sup>; <sup>1</sup>Safran Aircraft Engines; <sup>2</sup>NAAREA; <sup>3</sup>Institut Pprime/SP2MI; <sup>4</sup>Institut Pprime/Safran Tech; <sup>5</sup>Institut Pprime/ENSMA

Ni-based single crystal (SX) superalloys have a well-established history of application in high pressure turbine (HPT) blades and vanes. Nowadays, these components are increasingly being employed in the first stage of the low pressure turbine (LPT). As a result, aircraft engine manufacturers are facing new challenges arising from the design, manufacturing processes, evolving service conditions, and refurbishment requirements. Conventionally, the capability of Ni-based SX superalloys to withstand the harshest environments is related to a homogeneous cuboidal  $\gamma/\gamma'$  microstructure. However, future new applications have considered bimodal  $\gamma/\gamma'$  microstructures (presence of fine tertiary  $\gamma'$  precipitates 10-100 nm inside the  $\gamma$ -channels) resulting from either the manufacturing processes or from the routine use. This study investigates the resistance to the viscoplastic deformation of a 3<sup>rd</sup> generation Ni-based SX superalloy with a bimodal distribution of  $\gamma'$  precipitates. TEM observations showed presence of dislocations after heat treatment to achieve the bimodal microstructure. Even without plastic strain, dislocations were identified surrounding the secondary  $\gamma'$  precipitates. Stress relaxation and creep properties at 750 °C and 850 °C were very sensitive to such bimodal microstructure. Specimens with a bimodal  $\gamma'$  precipitation showed a creep life five to six times lower than the reference samples. According to the Norton's type diagram, rate controlling deformation mechanisms of the reference and bimodal microstructures appear to be same at both temperatures and under different initial conditions (with and without prior plastic strain), but with a higher strain rate for the bimodal microstructure.

### 11:45 AM

**Non-destructive Volumetric Methods for Detection of Recrystallized (RX) Grains in Single Crystal (SX) Aerospace Components:** *Iuliana Cernatescu*<sup>1</sup>; Chris Pelliccione<sup>2</sup>; Robert Koch<sup>3</sup>; Ryan Breneman<sup>4</sup>; Slade Stolz<sup>2</sup>; Venkat Seetharaman<sup>1</sup>; David Furrer<sup>2</sup>; <sup>1</sup>Pratt & Whitney

Single-crystal (SX) nickel-based superalloys are used as blade materials for gas turbine aircraft engines due to their superior mechanical and environmental performance. These properties of SX superalloys depend highly upon their crystallographic orientations. The SX superalloy components contain no large angle boundaries, which excludes intergranular oxidation and rupture. However, the industrial manufacturing of SX superalloy blades can still result in the formation of recrystallized (RX) grains which can significantly limit the life of these components. The RX grains can form anywhere within a SX blade but are most frequently observed in areas of high geometrical complexity. These are often areas where high thermal stresses occur during solidification and subsequent cooling processes due to significant mechanical constraint between shell/core materials and airfoil and can occur on the interior walls of hollow configurations. Focused research efforts have been conducted to develop and demonstrate a non-destructive method for volumetric analysis and detection of RX grains in SX components. This method is being further developed and deployed via an integrated computational materials engineering approach to further identify and control critical to quality material and processing parameters to mitigate such features in the most complex production castings. Implementation of this advanced non-destructive evaluation process will be reviewed in terms of targeted locations based on probabilistic material and process modeling.

### 12:10 PM

**Interfacial Strength Evaluation Between Sulfur-segregated Al<sub>2</sub>O<sub>3</sub> and Ni-Al Single Crystal Alloy Using Nanoindentation:** *Chihiro Tabata*<sup>1</sup>; Toshio Osada<sup>2</sup>; Takahito Ohmura<sup>2</sup>; Tadaharu Yokokawa<sup>2</sup>; Kyoko Kawagishi<sup>2</sup>; Shinsuke Suzuki<sup>1</sup>; <sup>1</sup>Waseda University; <sup>2</sup>National Institute for Materials Science

Ni-base superalloys have excellent oxidation resistance, but impurity S drastically decreases their properties. This is due to the segregation of S to the oxide/substrate interface, but direct and quantitative measurements of the interfacial strength in relation to the S segregation level have not been widely conducted. The objective of this research is to quantitatively analyze the interfacial strength between the Al<sub>2</sub>O<sub>3</sub> layer and Ni-base substrate interfacial strength, depending on the S segregation level, using nanoindentation. Ni-9.8 wt.% Al alloys were prepared by melting the material using either an Al<sub>2</sub>O<sub>3</sub> crucible (high S<sub>interface</sub> alloy) or a CaO crucible (low S<sub>interface</sub> alloy). Nanoindentation tests using a 60 degree pyramidal diamond indenter were conducted, and the cross-sections of both specimens exposed the (100) plane. Indentation near the interface formed cracks at the boundary between the two layers, which can be observed as pop-ins in the load-depth curves. The amount of load at the initial pop-in most likely represents the interfacial strength between the Al<sub>2</sub>O<sub>3</sub> layer and Ni-base substrate. A Weibull analysis of results showed that suppression of the S segregation level increased the critical  $\hat{a}$  scale parameter for crack formation by 650 iN. This suggests that we were able to successfully compare the effect of S segregation on the interfacial strength between the Al<sub>2</sub>O<sub>3</sub> layer and the Ni-base substrate quantitatively

12:35 PM

**A Coupled Numerical Scheme for Simulating Liquid Metal Cooling Process and its Validation:** Shengxu Xia<sup>1</sup>; Zhaofeng Liu<sup>2</sup>; Jianzheng Guo<sup>2</sup>; Yuzhang Lu<sup>3</sup>; Jian Zhang<sup>3</sup>; <sup>1</sup>Shenzhen Wedge Central South Research Institute Co., Ltd.; <sup>2</sup>State Key Laboratory of Powder Metallurgy, Central South University; <sup>3</sup>Institute of Metal Research, Chinese Academy of Sciences

The heat transfer dynamics in the Liquid Metal Cooling (LMC) process, aimed at the production of directionally solidified single crystal, is intricate due to the involvement of two primary heat exchange pairs: the interaction between the mold and the casting metal, and the interaction between the mold and its environment including liquid metal coolant and the furnace. Present numerical simulations face challenges especially in accurately capturing the temperature and flow field evolution within the coolant, resulting in potential inaccuracies in calculating the solidification process. In response to this, the current study proposes a coupled model designed to concurrently calculate the solidification process in a single crystal casting and simulate the temperature and flow fields within the coolant. This coupling is achieved through a mutual exchange of results, where the outcomes of each process serve as boundary conditions for the other. The computational results obtained from the coupled model are compared with experimental measurements taken within the casting and coolant (Sn), revealing a commendable level of agreement. Subsequently, the coupled model is applied to explore the influence of casting sizes and arrangements on temperature and flow of coolant. The simulations yield preliminary yet insightful findings, offering valuable information that may contribute to the optimization of the LMC process.

---

## General Session 7: Repair and Refurbishment

Wednesday AM | September 11, 2024  
Exhibit Hall | Seven Springs Mountain Resort

**Session Chairs:** Fernando Pedraza, Universite de La Rochelle; Iuliana Cernatescu, Pratt and Whitney

8:30 AM

**Improving Repair Braze Gap Strength Through the Development of a Novel Superalloy Filler:** Dirk Reker<sup>1</sup>; Roman Sowa<sup>2</sup>; Caspar Schwalbe<sup>3</sup>; Bernd Boettger<sup>4</sup>; Frank Seidel<sup>1</sup>; Marco Panella<sup>3</sup>; Kai Moehwald<sup>5</sup>; Martin Nicolaus<sup>5</sup>; Wolfgang Tillmann<sup>6</sup>; <sup>1</sup>MTU Maintenance Hannover; <sup>2</sup>MTU Aero Engines Polska; <sup>3</sup>MTU Aero Engines; <sup>4</sup>ACCESS e.V.; <sup>5</sup>Institute of Materials Science, Leibniz Universität Hannover; <sup>6</sup>Institute of Materials Engineering, TU Dortmund University

Superior repair technology is a principal driver for resource-effective operation in the aviation industry. Routine operation of aircraft engines exposes the turbine components to high stresses and high temperatures. To withstand extreme operational conditions Ni-based superalloys are used to manufacture turbine components. A crucial factor in targeting the assurance of repair reliability is improving the repair braze gap strength. This study seeks to improve the braze repair strength by optimising a novel superalloy filler material. The superalloy filler material acts as a complementary additive, that is blended with the braze alloy in powder form and improves the joint properties after brazing. The novel superalloy filler was developed by materials simulation using the CALPHAD (CALculation of PHase Diagram) approach. Phase field modelling using MICRESS® was applied to study the brazing kinetics and microstructure evolution. The developed superalloy filler was experimentally validated in respect to microstructure improvement and mechanical potential by tensile testing at elevated temperature (871 °C). The application of the novel superalloy filler shows an increase in ultimate tensile strength in comparison to a conventional braze blend.

8:55 AM

**Effect of Rejuvenation Treatment on SX Ni-based Superalloys Subjected to Low Cycle Fatigue:** Inmaculada López Galilea<sup>1</sup>; Anne Dennstedt<sup>2</sup>; Sebastian Weber<sup>1</sup>; Marion Bartsch<sup>2</sup>; <sup>1</sup>Ruhr University Bochum; <sup>2</sup>German Aerospace Center

Rejuvenation treatments with integrated hot isostatic pressing have been proven to re-establish the  $\gamma/\gamma'$  microstructure of single crystalline nickel-based superalloys after creep deformation, close porosity, and recover creep strength to a significant extent. Therefore, rejuvenation treatment is expected to be effective in extending the service life of components such as turbine blades for gas turbines resulting in reduced costs and improved sustainability compared to replacing the component. Since such components are subjected to combined creep-fatigue loading, this investigation is aiming to answer the question if a rejuvenation procedure, which has proved to recover single crystalline superalloys after creep, is effective in rejuvenating these materials after low cycle fatigue. For this purpose, test samples have been subjected after high temperature low cycle fatigue experiments to a rejuvenation procedure. The materials microstructure has been studied by non-destructive X-ray computer tomography before and after rejuvenation. Subsequently, metallographic sections were prepared from rejuvenated samples and investigated by scanning electron microscopy. Pores and precipitates detected in high resolution section images were identified in the reconstructed volume and used to fit the metallographic section images into this volume. Pores and cracks emanating at pores during fatigue testing were closed by rejuvenation as long as they were not connected to the surface. Electron back scatter diffraction performed on the sections revealed that, in contrast to creep samples, the fatigue samples were recrystallized during rejuvenation. It is concluded that fatigue damage cannot be reversed by the same rejuvenation procedure that is effective for creep damage.

9:20 AM

**High Temperature Fatigue Crack Growth in Nickel-based Alloys Refurbished by Additive Manufacturing:** Ashok Bhadeliya<sup>1</sup>; Birgit Rehmer<sup>1</sup>; Bernard Fedelich<sup>1</sup>; Torsten Jokisch<sup>2</sup>; Birgit Skrotzki<sup>1</sup>; Jürgen Olbricht<sup>3</sup>; <sup>1</sup>Federal Institute for Materials Research and Testing (BAM); <sup>2</sup>Siemens Energy Global GmbH & Co. KG

Hybrid additive manufacturing plays a crucial role in the restoration of gas turbine blades, where e.g., the damaged blade tip is reconstructed by the additive manufacturing process on the existing blade made of a parent nickel-based alloy. However, inherent process-related defects in additively manufactured material, along with the interface created between the additively manufactured and the cast base material, impact the fatigue crack growth behavior in bi-material components. This study investigates the fatigue crack growth behavior in bi-material specimens of nickel-based alloys, specifically, additively manufactured STAL15 and cast alloy 247DS. The tests were conducted at 950 °C with stress ratios of 0.1 and -1. Metallographic and fractographic investigations were carried out to understand crack growth mechanisms. The results revealed significant retardation in crack growth at the interface. This study highlights the potential contributions of residual stresses and microstructural differences to the observed crack growth retardation phenomenon, along with the conclusion from an earlier study on the effect of yield strength mismatch on crack growth behavior at a perpendicular interface in bi-material specimens.



9:45 AM

**The Effect of a Laser-based Heat Treatment on the Microstructure of a Superalloy After a Minimally Invasive Repair by Direct Energy Deposition:** Bernd Müller<sup>1</sup>; Gerhard Backes<sup>2</sup>; Wolfgang Kueppers<sup>3</sup>; Jochen Kittel<sup>3</sup>; Norbert Pirch<sup>3</sup>; Susanne Hemes<sup>4</sup>; Markus Pedersen<sup>5</sup>; Constantinos Hatzoglou<sup>5</sup>; Paraskevas Kontis<sup>5</sup>; <sup>1</sup>Rolls-Royce Deutschland Ltd & Co KG; <sup>2</sup>Dap RWTH; <sup>3</sup>Fraunhofer ILT; <sup>4</sup>Access e.V. Aachen; <sup>5</sup>NTNU Norwegian University

In this study, a laser-based heat treatment is applied on IN718 superalloy substrate repaired by a minimally invasive direct energy deposition process. The focus is on the laser-based heat treated microstructure, aiming to enable minimally invasive repair processes to take place either "on-wing" or "near-wing". Hardness measurements were performed on the as-repaired and heat treated microstructure, while electron microscopy, electron backscatter diffraction and atom probe tomography analyses were performed to investigate the microstructure. After the laser-based heat treatment, the hardness of the repaired part increased compared to the as-repaired and reached values similar to that of the substrate. Besides, microstructural analysis unveiled non-uniform  $\gamma''$  precipitate formation, linked to observed micro-segregation from the repair process persisting post-heat treatment. Precipitation-free areas were observed while co-precipitation of  $\gamma''$  and  $\gamma'$  in duplet and triplet particles was infrequent. Interdendritic areas exhibited Laves phases regions with needle-shaped  $\delta$  precipitates forming directly from the Laves phase. Carbonitrides coexisted with Laves phase, creating complex Laves regions. Although a single-step heat treatment will not lead to a complete dissolution of the undesirable microstructure features, a solution treatment step using the same minimally invasive equipment can unlock the full potential of in-situ maintenance through laser-based heat treatments.

---

## Interactive Session D: Repair & Disk Alloy Manufacture

Wednesday AM | September 11, 2024  
Winterberry | Seven Springs Mountain Resort

---

**D-1: Effect of Incremental Deformation Path on the Microstructural Evolution of the  $\gamma$ - $\gamma'$  Nickel-Based Superalloy René 65:** Theo Huyghe<sup>1</sup>; Lucie Le Sache<sup>2</sup>; Eric Georges<sup>3</sup>; Daniel Pino Munoz<sup>1</sup>; Julien De Jaeger<sup>4</sup>; Christian Dumont<sup>3</sup>; Nathalie Bozzolo<sup>1</sup>; <sup>1</sup>CEMEF Mines Paris; <sup>2</sup>Safran Aircraft Engines; <sup>3</sup>Aubert & Duval; <sup>4</sup>Safran Tech

The focus of this study is on the microstructural evolution of the  $\gamma$ - $\gamma'$  nickel-based superalloy René 65 under monotonic and incremental deformation paths. Here, incremental deformation is defined as the alternation of small deformations and short dwell times, representing the deformation path processed during a ring rolling. Incremental and monotonic deformation paths are performed using hot torsion and hot compression experiments and their resulting microstructures are compared. For a given final strain, strain rate and temperature, a monotonic deformation generates a higher fraction of recrystallization than an incremental deformation path does, for both torsion and compression experiments. Further experiments on interrupted incremental and monotonic compression deformation conditions are conducted to better understand the impact of dwell time on recrystallization. Static recovery and  $\gamma'$  precipitation evolution are two potential microstructural mechanisms discussed in this paper that could occur during dwell time and slow down the recrystallization evolution for incremental deformation conditions.

**D-2: Gamma Prime Precipitation in the Cast and Wrought AD730 Superalloy:** Jerome Blaizot<sup>1</sup>; Laurane Finet<sup>1</sup>; Aurelien Chabrier<sup>1</sup>; Alexandre Fornara<sup>1</sup>; Matthieu Fage<sup>1</sup>; Roufeida Remichi<sup>1</sup>; Mickael Dade<sup>2</sup>; Michel Perez<sup>3</sup>; <sup>1</sup>Aubert & Duval; <sup>2</sup>ERAMET; <sup>3</sup>Université de Lyon

AD730® is a  $\gamma/\gamma'$  polycrystalline superalloy which has been recently developed for future engine turbine discs. The  $\gamma'$  precipitation influences mechanical properties at the service temperature but also the kinetics of recrystallization during forging process. Consequently, a deep understanding and monitoring of  $\gamma'$  precipitation is required at each stage of the industrial process. The objective of this work is to understand the precipitation mechanism, determine the evolution of  $\gamma'$  size during cooling and isothermal heat treatments, and calibrate a model for the nucleation and growth of  $\gamma'$  during the ingot-to-billet conversion. The experimental analysis showed that water quenching at a cooling rate of 100 °C/s after a solution treatment at 1160 °C led to a fine and homogeneous  $\gamma'$  precipitation for which the average circle radius ranges from 10 nm to 20 nm. Then, samples were heat treated between 1000 °C and 1080 °C with various holding times to characterize and quantify the size of precipitates. The results were compared to the precipitation modeling using the in-house software PreciSo, a multi-class, Kampmann-Wagner Numerical precipitation model based on classical nucleation and growth theories. Even if the simulations of precipitation during isothermal heat treatments start with the correct initial radius, coarsening appears to occur slower than predicted by the simulations. This discrepancy is attributed to one simulation parameter, the diffusivity of solute elements, which needs to be improved to obtain a better fit with experimentations.

**D-3: Modeling of Powder Metallurgy Hot Isostatic Pressing and Application to Ni-base Superalloy:** Swapnil Patil<sup>1</sup>; Alon Mazar<sup>2</sup>; Nathan Almirall<sup>2</sup>; Christopher McLasky<sup>2</sup>; Vipul Gupta<sup>2</sup>; Kai Lorcharoensery<sup>3</sup>; Nicholas Krutz<sup>3</sup>; Justin Bennett<sup>3</sup>; Timothy Hanlon<sup>2</sup>; <sup>1</sup>GE Aerospace Research, Bangalore; <sup>2</sup>GE Aerospace Research, Niskayuna; <sup>3</sup>GE Aerospace, Cincinnati

A finite element (FE) model was developed to simulate the densification of a nickel-base superalloy powder during the hot isostatic pressing (HIP) process. A unified material model which simultaneously captures the various deformation mechanisms, such as plasticity and creep, was used in this study. Elaborate experiments were carried out to generate thermal and mechanical properties and calibrate the model parameters for an aerospace industry relevant powder alloy. FE simulations of powder encapsulated in a stainless-steel canister were performed to evaluate the model capability to capture the canister distortion as well as powder densification during the HIP process. The densification and shape change predictions from the FE model were verified using experimental data obtained from interrupted HIP runs performed at various temperatures and pressure ramp rates. Good agreement was found between the model predictions and the experimental results. It was found that including the creep response of the canister in the simulation had a significant influence on the capability of the FE model to predict the powder densification behavior, especially during the hold time at peak pressure. The FE model provided critical insights on mechanical factors leading to non-uniform densification in the powder compact and canister deformation.

**D-4: On the Formation of Multiply Coherent  $\gamma$  Grains in a Powder Metallurgy Ni Base Superalloy:** *Yonguk Lee*<sup>1</sup>; Cameron Hale<sup>1</sup>; Eric Payton<sup>2</sup>; Victoria Miller<sup>1</sup>; <sup>1</sup>University of Florida; <sup>2</sup>University of Cincinnati

In this study, a unique microstructure with  $\gamma$  grains which contain with multiple coherent primary  $\gamma'$  particles is reported. We term these unique features "multiply coherent grains" (MCGs). While the grains containing coherent primary  $\gamma'$  particles suggests the heteroepitaxial recrystallization (HeRX) mechanism, HeRX can only explain the presence of a single coherent primary  $\gamma'$ , not multiple. Other potential formation mechanisms for the MCGs are examined, and a formation mechanism based on a special case of Smith-Zener pinning-unpinning is proposed. The implications of the proposed mechanism on grain size evolution are discussed.

**D-5: Using "Microstructure Informatics" to Understand Abnormal Grain Growth Factors in Powder Metallurgy Ni-based Superalloys:** *Luis Arciniaga*<sup>1</sup>; Pascal Thome<sup>1</sup>; Kevin Severs<sup>2</sup>; Sammy Tin<sup>1</sup>; <sup>1</sup>University of Arizona; <sup>2</sup>ATI Forged Products

Advanced electron back scatter diffraction (EBSD) and electron dispersive spectroscopy (EDS) techniques were used to systematically quantify meso-scale microstructural descriptors in an advanced powder processed polycrystalline Ni-base superalloy containing elevated levels of refractory alloying additions. The microstructural changes of the alloy as a function of effective strain were tracked and related to the subsequent heat-treated microstructures. This emerging field of "microstructure informatics" extends beyond the conventionally used metrics of grain and precipitate sizes and distributions. Due to the multidimensional nature of the data, manual microstructure characterization becomes virtually impossible, especially when a multitude of different material states must be considered. This motivated the development of an automated microstructure characterization procedure, which extracts useful geometric, crystallographic, and chemical microstructure features through a batch process. These features provide a level of microstructure detail that has not traditionally been demonstrated at a statistically significant scale capable of effectively capturing the level of intrinsic heterogeneity that is present in polycrystalline Ni-base superalloys. In this study, microstructural descriptors from the deformed material were evaluated and used to understand the grain growth response during super-solvus heat treatment. Compared to traditional qualitative and semi-quantitative approaches for characterizing microstructures, the innovative methodology used in this investigation provide insightful, quantitative microstructure metrics that lead to the generation of new knowledge and scientific understanding.

**D-6: Analysis of the Recovery Potential Through Repair of Key Tensile Properties for a Second Generation Ni-based SX Superalloy Exposed to Simulated Routine Service Conditions:** *Marco Panella*<sup>1</sup>; Liren Zheng<sup>2</sup>; Magdalena Futoma<sup>3</sup>; Caspar Schwalbe<sup>1</sup>; Dominique Eyidi<sup>2</sup>; Patrick Villechaise<sup>2</sup>; Jonathan Cormier<sup>2</sup>; <sup>1</sup>MTU Aero Engines AG; <sup>2</sup>Institut Pprime, UPR CNRS 3346; <sup>3</sup>MTU Aero Engines Polska Sp. z o.o.

Nickel-based single-crystal turbine components used for aero-engine turbine blades are exposed to cycles of temperature and stress during routine service. High temperature exposure (exceeding about 950 °C) results in a transformation of the precipitation from cuboidal to coarsened morphology. The coarsened microstructure has a detrimental effect on the mechanical properties and, therefore, lifespan of the component. In the present study, simulated service conditions (approximated by non-isothermal creep tests) were applied to SC2000 specimens. The effects of the non-isothermal creep deformation and a rejuvenation heat treatment on the alloy's microstructure and tensile and creep properties was analyzed. Non-isothermal creep tests were performed with a base temperature of 900 °C and a peak temperature of 1100 °C. SEM analysis confirmed a quick deterioration of the microstructure exposed to the simulated service coupled with a marked dislocations activity around the precipitates. In order to restore the initial properties, a super-solvus rejuvenation heat treatment was applied after deformation. The rejuvenation process successfully restored the initial precipitates morphology and the yield strength, while no improvement in creep properties was observed. Hypotheses and investigations are presented to explain this effect.

**D-7: Mechanical Properties of Waspaloy Repaired by Laser Metal Deposition and Cold Metal Transfer:** *Alice Cervellon*<sup>1</sup>; Marjolaine Sazerat<sup>2</sup>; Romain Bordas<sup>2</sup>; Lucie Barot<sup>3</sup>; Sophie Gillet<sup>1</sup>; Azdine Nait-Ali<sup>2</sup>; Patrick Villechaise<sup>2</sup>; Roland Fortunier<sup>3</sup>; Jonathan Cormier<sup>2</sup>; <sup>1</sup>Safran Aircraft Engines; <sup>2</sup>Institut Pprime - ENSMA; <sup>3</sup>LTDS - ENISE

The microstructure and mechanical properties of additively manufactured Waspaloy were characterized in the industrial context of refurbishment. Two processes were studied to discuss their advantages and drawbacks considering the targeted application: Laser Metal Deposition with powder and Cold Metal Transfer. The resultant microstructures were compared in the build-up and at the interface between the wrought base Waspaloy and the additively manufactured part, in the as-built condition and after post weld heat treatments. Tensile and creep properties were studied along three directions - horizontal, vertical and at the interface - to assess the anisotropy of the build-up and the strength of the interface/Heat Affected Zone induced by the metal deposition. Results show that both processes have limited anisotropy in the conditions studied, even though Cold Metal Transfer presents an important crystallographic and microstructural texture. Depending on the process used and heat treatments applied, the interface/Heat Affected Zone may not be the weakest point of the repaired part despite a neat interface. High temperature creep results also suggest that post weld heat treatments may not be necessary if this is the primary design criteria. Tensile properties of Cold Metal Transfer Waspaloy are highly dependent on the deposit thickness from where the specimens are extracted, due to an in-situ heat treatment that takes place during production of large deposits. The different results are discussed considering the limitations of industrial repair operations such as metal costs, deposition rate, repaired volume and targeted application.

**D-8: Spark Plasma Diffusion Bonding of Inconel 718 Superalloys by Using Atomic Cluster Powder Fillers:** Zhen Zhang<sup>1</sup>; Yunting Li<sup>1</sup>; Peng Peng<sup>1</sup>; Maodong Kang<sup>1</sup>; Jun Wang<sup>1</sup>; <sup>1</sup>Shanghai JiaoTong University

Brazing-repair of nickel-based superalloy precision casting has attracted a wide concern as the issues related to hot cracking, dimensional deformation and loss of strengthening phase have not been solved for a long term. In this study, we proposed to use atomic cluster powder filler which was manufactured through mechanical ball-mixing of Ni atomic cluster nanoparticles with Inconel 718 powders to achieve a well-bonded joint. Spark plasma diffusion bonding was conducted to evaluate the atomic cluster powder fillers and Inconel 718 powder fillers counterpart. The microstructure and mechanical properties of bonding joints were investigated to explore the effects of atomic cluster nanoparticles on bonding-repair of superalloys. It was found that the Ni atomic cluster nanoparticles were uniformly distributed into Inconel 718 powders. The joint of atomic cluster powder fillers exhibited a higher densification increased by 42% compared with Inconel 718 powder fillers. The tensile mechanical properties of bonded sample will be dependent on the bonding interface quality rather than microstructure of joint region. The atomic cluster powder fillers resulted in a comparable yield strength of bonded sample with 200 K lower bonding temperature compared with Inconel 718 powder fillers.

---

## General Session 8: Disk Alloy Manufacture

Wednesday AM | September 11, 2024  
Exhibit Hall | Seven Springs Mountain Resort

**Session Chairs:** Satoshi Utada, National Institute for Materials Science; Sammy Tin, University of Arizona

---

### 11:20 AM

**Methods for Characterising Oxide Inclusions & Porosity in Powder Ni Alloys for Disc Rotor Applications:** Mark Hardy<sup>1</sup>; <sup>1</sup>Rolls-Royce Plc

Oxide inclusions and porosity are present in nickel alloys that are made using powder metallurgy. Both features can nucleate fatigue cracks. Surface oxide inclusions can significantly reduce fatigue lives. This is evident if lives are compared to those for crystallographic cracks that develop from slip bands, which are characterized by facets on fracture surfaces. Pores mainly occur from trapped gas in powder particles, whereas inclusions typically arise from melting the alloy and from powder manufacture. Since most inclusions are too small to be detected from ultrasonic inspection, probabilistic lifing assessment is required to ensure the risk of failure from "melt anomalies" in disk rotors is acceptably low. Such calculations apply a mathematical description of inclusion size and frequency. This paper examines methods for characterizing size and frequency of oxide inclusions and porosity from powder and billet material, which includes material that contains oxide inclusions or "seeds" that were added intentionally to understand fatigue behavior. Large bar tensile (LBT) testing of billet material was found to be the most capable method for characterizing inclusion size. However, rate of occurrence information cannot be measured directly; it must be implied by fitting inclusion size data to probability functions. Given uncertainties with this approach, a method has been devised to measure rate of occurrence directly. Inspections of polished surfaces of billet material have been shown to be viable for production use. Porosity of a coarse powder fraction has been characterized by mounting powder in resin so that automated image capture and analyses could be undertaken on polished surfaces. Finally, the sizes of the very low frequency of larger inclusions, which are detected by ultrasonic inspection of billet, have been characterized from electron microscopy on polished surfaces.

### 11:45 AM

**Effect of Strain Rate on Dynamic Recrystallization of a Typical  $\gamma$ - $\gamma'$  Nickel-Based Superalloy with Initial Bimodal Precipitation:** Federico Orlacchio<sup>1</sup>; Daniel Pino Munoz<sup>2</sup>; Madeleine Bignon<sup>2</sup>; Chi-Toan Nguyen<sup>1</sup>; Ilusca Soares Janeiro<sup>2</sup>; Marc Bernacki<sup>2</sup>; Nathalie Bozzolo<sup>2</sup>; <sup>1</sup>SAFRAN; <sup>2</sup>MINES ParisTech PSL -Research University, CEMEF - Centre de Mise en Forme des Matériaux, CNRS UMR 7635

The effect of strain rate on microstructure evolution of a  $\gamma$ - $\gamma'$  nickel-based superalloy during hot deformation has been examined in this study. The experiments were conducted below the  $\gamma'$  phase solvus temperature, at 1050 °C with various strain rates ( $10^{-1}$ ,  $10^{-2}$ , AND  $10^{-3}$  S<sup>-1</sup>) up to different macroscopic strain level (0.2, 0.8 and 1.3). An inverse effect of strain rate on dynamic recrystallization has been observed with an increase in the recrystallized fraction as strain rate increases, for a fixed macroscopic strain level. Scanning electron microscope and electron backscattered diffraction analysis were employed to investigate the deformed microstructures in terms of  $\gamma$  phase evolution and  $\gamma'$  precipitation state. A constant average size value of recrystallized grains at 1  $\mu$ m is obtained for all tested conditions, suggesting that nucleation of new dynamically recrystallized grains is favored at the expense of the growth of recrystallized grains during hot deformation, which is inhibited. Furthermore, the complete absence of fine  $\gamma'$  precipitation within dynamically recrystallized grains, reveals a strong interaction between the progress of recrystallization front and the presence of fine  $\gamma'$  precipitates.

### 12:10 PM

**Precipitation of  $\gamma\gamma'$  in Two  $\gamma\gamma$ - $\gamma'$  Ni-based Superalloys During the Solvus Transition Stage of Ingot to Billet Conversion; Effects on  $\gamma$  Grain Structure and Implications for Open Die Forging:** Angus Coyne-Grell<sup>1</sup>; Marcos Pérez<sup>1</sup>; Ioannis Violatos<sup>1</sup>; Jérôme Blaizot<sup>2</sup>; Christian Dumont<sup>2</sup>; Sebastien Nouveau<sup>2</sup>; <sup>1</sup>University of Strathclyde; <sup>2</sup>Aubert et Duval

Udimet®720Li and AD730@UDIMET is a registered trademark of Special Metals Corporation. AD730 is a registered trademark of Aubert & Duval are  $\gamma$ - $\gamma'$  Ni-based superalloys manufactured through casting and wrought processing, i.e. using ingot-to-billet conversion. These alloys are intended for use in safety critical aeroengine components, and there are strict requirements on the microstructural characteristics they must achieve at the end of the conversion process. Conventional ingot-to-billet conversion is an expensive and complex process, requiring multiple open-die forging operations and reheating steps to achieve a homogeneous microstructure. A main goal of this conversion process is to refine the as-cast grain structure, which comprises grains centimetres in size, down to a grain size of approximately 20  $\mu$ m. The present work studies the microstructural evolution of Udimet 720Li and AD730 billet material at the "solvus transition" stage of the conversion process, i.e. the controlled cooling through the solvus temperature. The formation of  $\gamma'$  prime precipitates during controlled cooling from supersolvus temperatures, and their interaction with the grain structure is the focus of this work. It is shown that the size and morphology of the grains in both alloys are significantly affected by discontinuous precipitation during cooling through the solvus temperature, and a method to exploit this during industrial ingot-to-billet conversion is suggested.

12:35 PM

**Full-field Microstructure Modeling During Forging a Polycrystalline  $\gamma$ - $\gamma'$  Nickel-based Superalloy:** *Chi-Toan Nguyen*<sup>1</sup>; Daniel Galy<sup>1</sup>; Jean-Michel Franchet<sup>1</sup>; Jérôme Blaizot<sup>2</sup>; Christian Dumont<sup>2</sup>; Lucie Le Saché<sup>1</sup>; Julien de Jaeger<sup>1</sup>; Baptiste Flipon<sup>3</sup>; Nathalie Bozzolo<sup>3</sup>; Marc Bernacki<sup>3</sup>; <sup>1</sup>Safran; <sup>2</sup>Aubert & Duval; <sup>3</sup>CEMEF

The present paper demonstrates great capability of the full-field finite element DIGIMU® software included recrystallization models to simulate the microstructure evolution during forging an industrial part in René 65, a  $\gamma$ - $\gamma'$  nickel-based superalloy. The macroscopic forging conditions simulated by the finite element FORGE® software were used as the thermo-mechanical inputs of the microstructure simulations in the DIGIMU® software. The recrystallization models in the DIGIMU® software were calibrated from torsion tests on laboratory-scale samples at sub-solvus and super-solvus temperatures from 1000 °C to 1150 °C and at strain rates ranging from  $10^{-2}$  to  $0.75 \text{ s}^{-1}$ . The calibrated model is able to predict, correctly, the mean and distribution of grain sizes in different deformation conditions of laboratory-scale samples and, more importantly, for eight different positions of interest in an industrial part forged by multiple operations at sub-solvus temperatures and followed by a solution heat treatment. The differences between the predicted and experimental average grain sizes are in the range of 0.5 to 1.0 ASTM (which is around 1.5 to  $3.0 \mu\text{m}$  difference when comparing to the experimental grain size of 10 ASTM  $\sim 11 \mu\text{m}$ ). The model will help with understanding and optimizing of forging processes to achieve desirable microstructures and, in turn, the mechanical properties of aircraft engine forged components.

---

## General Session 9: Additive Manufacturing I

Wednesday PM | September 11, 2024  
Exhibit Hall | Seven Springs Mountain Resort

**Session Chairs:** Yuanbo Tang, University of Birmingham; Timothy Smith, NASA Glenn Research Center

6:30 PM

**A Physics-based, Probabilistic Modeling Approach to Design, Manufacture, and Certify AM Components:** *David Furrer*<sup>1</sup>; Masoud Anahid<sup>2</sup>; S. Burlatsky<sup>2</sup>; Manish Kamal<sup>1</sup>; <sup>1</sup>Pratt & Whitney; <sup>2</sup>Raytheon Technologies

Additive manufacturing (AM) has captured the imagination of many in the materials, manufacturing and design communities. While AM has shown significant potential to produce complex geometries from a wide range of materials, the stringent requirements of production components necessitate advances in the way components are designed, manufactured, and certified. Dynamic properties of AM components are known to be significantly hindered by the presence of build defects. An integrated computational materials engineering (ICME) approach to AM has been pursued through which build defects can be accurately predicted on a component location-specific basis. This capability is leading to a model-based material definition (MBMD) approach to process design and control, and subsequent component qualification and certification. The development and demonstration of component and process manufacturing design examples of this approach for a nickel-base superalloy case application will be provided.

6:55 PM

**3D Characterization of Defects and Microstructure in High Density LPBF Prints of a CoNi Alloy:** *James Lamb*<sup>1</sup>; Evan Raeker<sup>1</sup>; Kira Pusch<sup>1</sup>; McLean Echlin<sup>1</sup>; Stephane Forsik<sup>2</sup>; Ning Zhou<sup>2</sup>; Austin Dicus<sup>2</sup>; Tresa Pollock<sup>1</sup>; <sup>1</sup>University of California Santa Barbara; <sup>2</sup>Carpenter Technology Corporation

Laser powder bed fusion (LPBF) printing defects are investigated through multimodal 3D serial sectioning data on a model CoNi alloy. Defect segmentation across three different LPBF prints with different scan strategies, in which interlayer rotation and the presence of a contour scan is varied, reveal fully dense microstructures (>99.8% dense). Despite being in a density range commonly considered as fully dense material, these prints contain an array of small pores, lack-of-fusion defects, and cracks that can be highly anisotropic. Their size and number are compared to those found in conventional superalloy casting techniques (investment casting, single crystal Bridgeman casting). In the AM samples, most pores and cracks have a thickness on the order of 3-6  $\mu\text{m}$ , beyond the resolution capabilities of most industrial non-destructive evaluation techniques. A comparison between 3D and 2D defects measurements is included, revealing significant variability between 2D measurements and the ground truth 3D data. A state-of-the-art machine learning framework, U-Net, is implemented for defect segmentation within three TriBeam tomography datasets containing backscattered electron images with variable contrast conditions. U-Net results indicate high fidelity defect segmentation within all three datasets where recall and precision are >85%. The 3D reconstructions of the CoNi alloy samples provide insight into the defect content that can be expected from high-quality fully dense LPBF printed superalloy material.

7:20 PM

**The Relationship Between Strain-age Cracking and the Evolution of  $\gamma'$  in Laser Powder-Bed-Fusion Processed Ni-based Superalloys:** *Jonathon Markanday*<sup>1</sup>; Neil D'Souza<sup>2</sup>; Nicole Church<sup>1</sup>; James Miller<sup>1</sup>; Jessica Pitchforth<sup>1</sup>; Leigh Connor<sup>3</sup>; Stefan Michalik<sup>3</sup>; Bryan Roebuck<sup>4</sup>; Nicholas Jones<sup>1</sup>; Katerina Christofidou<sup>5</sup>; Howard Stone<sup>1</sup>; <sup>1</sup>University of Cambridge; <sup>2</sup>Rolls-Royce; <sup>3</sup>Diamond Light Source; <sup>4</sup>National Physical Laboratory; <sup>5</sup>University of Sheffield

Factors affecting strain-age cracking (SAC) have been quantitatively assessed in a range of Ni-base superalloys with differing contents. Differences in the amount of present in the as-built condition of HA282, STAL 15DE, CM247LC and IN713LC are highlighted. In the as-built condition, are absent in HA282, but appear as nano-clusters in IN713LC. On heating, precipitates coherently in the phase, increasing the yield strength. The kinetics of precipitation are dependent on the heating rate and precipitation terminates at different temperatures in different alloys. The propensity to SAC is assessed via volume changes accompanying precipitation, increase in elastic modulus accompanying precipitation and a loss in ductility/grain boundary cohesive strength with increasing temperature. A marked feature of additively built microstructures is the dramatically low grain boundary cohesive strength at 800 C, which is related to the segregation within the terminal liquid film at the grain boundary. The most important factor contributing to SAC is the lack of ductility and reduced grain boundary cohesive strength.

## Interactive Session E: Additive Manufacturing & Environmental Behavior

Wednesday PM | September 11, 2024  
Winterberry | Seven Springs Mountain Resort

### E-1: Beyond Hot Cracking: Impact of Minor Elements on a Novel Ni-based Superalloy for Additive Manufacturing: *Kai Dörries*<sup>1</sup>;

Christoph Haberland<sup>2</sup>; Juri Burow<sup>3</sup>; Joachim Rösler<sup>1</sup>; Bodo Gehrman<sup>3</sup>; Christina Somsen<sup>3</sup>; Sebastian Piegert<sup>2</sup>; Håkan Brodin<sup>2</sup>; <sup>1</sup>TU Braunschweig; <sup>2</sup>Siemens Energy Global GmbH & Co. KG; <sup>3</sup>VDM Metals International GmbH

Minor elements such as boron, carbon, and zirconium have been used for many decades to improve the high-temperature properties of Ni-based superalloys. However, the advances in additive manufacturing technologies and the resulting popularity have put these elements in a bad light since they have been identified to be the major cause of hot cracking problems. This study covers the influence of these elements on hot cracking but its focus lays on their impact on strain-age cracking (SAC) and mechanical properties. The impact of these elements has been studied in four versions of a high tantalum-containing novel Ni-based superalloy that is being developed for Powder Bed Fusion-Laser Beam/Metals (PBF-LB/M). Increasing the boron content from 0.007 wt.% to 0.019 wt.% leads to severe hot cracking, but reduces SAC during the heat treatment. The addition of 0.022 wt.% zirconium does not increase the hot cracking susceptibility but increases the SAC susceptibility. The variation of minor elements does not affect room temperature tensile properties, but an increased zirconium and boron content increases the elongation at fracture at 850°C. The alloys with a low boron and medium boron content show a high notch-sensitivity during stress-rupture tests, which leads to failure in the fillet of the sample. Only the boron and zirconium alloys were able to achieve valid stress-rupture results.

### E-2: Concurrent Improvement of Additive Manufacturing Processability and Creep Performance in a Legacy Polycrystalline Superalloy Using Grain Boundary Strengtheners: *A Shaafi Shaikh*<sup>1</sup>;

Eduard Hryha<sup>1</sup>; Mohammad Sattari<sup>1</sup>; Mattias Thuvander<sup>1</sup>; Kevin Minet-Lallemant<sup>2</sup>; <sup>1</sup>Chalmers University of Technology; <sup>2</sup>EOS Metal Materials

Microcracking during processing and underperformance in creep have limited wider adoption of high  $\gamma'$ -fraction superalloys in additive manufacturing (AM). Certain processing issues are now understood to be related to solidification cracking caused by elements such as B and Zr, that are also essential for creep performance, particularly with fine-grained AM microstructures. A legacy  $\gamma'$ -strengthened polycrystalline superalloy 738LC was the subject of the current investigation. Printing trials conducted with the legacy composition and a modified version with 10 times the initial B content revealed extensive micro-cracking in the legacy composition, whereas the modified alloy produced a dense crack-free microstructure. CALPHAD-based solidification simulations and cracking susceptibility index calculations were performed to attempt to rationalise these findings. After hot isostatic pressing (1120 °C, 200 MPa, 4 hours) and ageing heat treatment (850 °C, 24 hrs), stress rupture tests showed an improvement in the rupture life of the modified alloy. Samples perpendicular to the AM building direction (typically the weaker orientation) showed a 50 % increase in rupture life compared to the conventional composition, and rupture ductility was also enhanced. Elevated temperature tensile ductility in the perpendicular direction increased to 11 El% for the modified alloy versus 6 El% for the conventional composition. These improvements are attributed to the presence of fine boride precipitates at grain boundaries of the modified alloy. The findings indicate that increasing the grain boundary strengthening element content may be a potential solution for both processing and mechanical performance issues in this superalloy.

### E-3: Improving the Additive Manufacturing Processability of a $\gamma'/\gamma'$ Cobalt-based Superalloy Through Tailored Chemical Modifications Without Degrading Hot Mechanical Properties: *Thibaut Froeliger*<sup>1</sup>;

Didier Locq<sup>1</sup>; Louise Toulbi<sup>1</sup>; Thomas Elcrin<sup>2</sup>; Rémy Dendievel<sup>3</sup>; <sup>1</sup>ONERA; <sup>2</sup>AddUp; <sup>3</sup>CNRS, SIMaP

This study aims to optimize the content of minor elements (C, B, Zr, Si, Hf) to enhance the manufacturability of  $\gamma'/\gamma'$  cobalt-based superalloys by additive manufacturing without degrading hot mechanical properties or oxidation resistance. Results show that reducing the amount of minor elements improves resistance to liquid phase cracking during additive manufacturing. However, removing these elements leads to a degradation of grain boundary strength or a reduction in the efficiency of the protective oxide layer at high temperatures. To reconcile these different aspects, the contents of minor elements are adjusted in a  $\gamma'/\gamma'$  cobalt-based superalloy following the study of its solidification path. The chemical modifications enable the development of various crack-free microstructures by directed energy deposition, which is unattainable before the chemical modifications. Creep and cyclic oxidation testing show that these chemical modifications do not affect the initial properties of the superalloy.

### E-4: Influence of the $\gamma'/\gamma'$ Misfit on the Strain-age Cracking Resistance of High- $\gamma'$ Ni and CoNi Superalloys for Additive Manufacturing: *Stephane Forsik*<sup>1</sup>;

Austin Dicus<sup>1</sup>; Gian Colombo<sup>1</sup>; Tao Wang<sup>1</sup>; Mario Epler<sup>1</sup>; Eamonn Connolly<sup>2</sup>; Jiraphant Srisuriyachot<sup>3</sup>; Alexander Lunt<sup>3</sup>; Ning Zhou<sup>1</sup>; <sup>1</sup>Carpenter Technology Corporation; <sup>2</sup>Diamond Light Source; <sup>3</sup>University of Bath

A series of new printable Ni and CoNi high  $\alpha'$  superalloys designed for additive manufacturing have been evaluated for strain-age cracking (SAC) resistance. Printability studies and heat treatment experiments were conducted to identify processing windows and characterize the overall resistance to SAC. High-resolution synchrotron X-Ray diffraction experiments were performed to measure the  $\alpha'$  and  $\alpha''$  lattice parameters as a function of the temperature. All the superalloys tested were found to have a positive  $\alpha'/\alpha''$  misfit at room temperature which decreases as the temperature increases. The misfit of a SAC-prone alloy, 247LC, decreases rapidly and turns negative at about 600 °C, whereas the misfit of superalloys with intermediate resistance to strain-age cracking remains slightly positive. In the three most SAC-resistant superalloys, the misfit remains larger than 0.05 % until at least 883 °C. The results show that a critical aspect for designing SAC-resistant alloys is ensuring that the misfit between  $\alpha'$  and  $\alpha''$  remains positive at all temperatures to generate compressive stresses on grain boundaries. Furthermore, the work also highlights a critical positive misfit value of 0.05% to prevent cracking.

### E-5: Microstructural Evolution and Thermal Stability of Additively Manufactured XH67 Nickel-based Superalloy: *Nithin Baler*<sup>1</sup>;

Indu Kollapalli<sup>1</sup>; Subhradeep Chatterjee<sup>2</sup>; *Dheepa Srinivasan*<sup>1</sup>; <sup>1</sup>PWRDC; <sup>2</sup>IIT Hyderabad

A new high strength nickel-based superalloy, XH67, has been fabricated by the laser powder bed fusion process (LPBF). Novel heat treatments via direct aging, solutionizing and aging, were carried out and compared with the as printed alloy, to study the evolution of phase equilibria and bring out the optimum mechanical properties of high strength and good ductility. A strengthened alloy, XH67 shows a high strength of 1040 MPa with a 25 % ductility, after direct aging (size of 10-30 nm and a volume fraction of 25-30 %). The as-printed structure with a cellular-dendritic morphology was retained during direct aging heat treatment contributing to the strength by Hall-Petch strengthening along with precipitation hardening by  $\gamma'$  precipitates. Discontinuous precipitation along the cell boundaries was a unique microstructural feature that are observed in the present alloy. Annealing twins were seen after solution and aging along with coarsening of the precipitates up to 50 nm. Thermodynamic calculation (Thermo-Calc) was used to validate the observed phase evolution as a function of heat treatment.

**E-6: Microstructure-mechanical Properties of Short-cycle Heat Treated Additively Manufactured Mar-M 509 Cobalt Superalloy:** Naimish Shah<sup>1</sup>; Rohit K. Yadav<sup>2</sup>; Dheepa Srinivasan<sup>1</sup>; *Nagamani Jaya Balila*<sup>2</sup>; <sup>1</sup>Pratt & Whitney Research and Development Center; <sup>2</sup>Indian Institute of Technology Bombay

Additively manufactured Mar-M 509, a cobalt-based superalloy, was evaluated for its microstructure and tensile behavior (at room temperature and 650 °C) after short cycle heat treatments, along the two orientations, longitudinal (L) and transverse (T) to the build direction. The microstructural evolution after single step heat treatments at 950 °C, 1150 °C and 1250 °C for 3 h was characterized using transmission electron microscopy. The alloy comprises a columnar-cellular dendritic microstructure strengthened by MC carbides forming a network along the cell boundaries in the as-printed condition. On heat treatment, the microstructure was characterized by the precipitation of M23C6 along with MC carbides. The T orientation showed higher yield strength and lower elongation than L for all the conditions. Amongst these, the 1150 °C heat treatment showed the optimum combination of yield strength and elongation (850 MPa, 20 %), attributed to the presence of fine MC carbides along the cell boundaries and coarse M23C6 carbides at the grain boundaries, with a carbide fraction of nearly 18%. At the test temperature of 650 °C, the optimum yield strength of ~740 MPa and elongation of 21 % was seen in the 950 °C HT condition. This understanding of microstructure-mechanical property correlation for a palette of short cycle ageing treatments thus allows for choosing the right combination for the desired application.

**E-7: Reinventing H230 Alloy Through Additive Manufacturing with Breakthrough Performance Gain:** *Youping Gao*<sup>1</sup>; <sup>1</sup>Castheon Inc

By controlling additive manufacturing process, particularly Laser Powder Bed Fusion process, significantly different microstructure and constituents' formation and distribution can be achieved robustly for superior materials properties gain without altering the bulk materials chemistry. Furthermore, a supersaturated solid solution structure can be obtained without solution treatment and subsequent quench operation to attain optimized properties by forming a high-volume fraction and uniformly distributed fine strengthening phase. In this study, fine and stable carbides for Carbide Dispersive Strengthening (CDS) to improve not only general materials properties but more critically to provide strengthening mechanisms above  $\gamma'$  solvus temperature for extreme environment applications such as hypersonic leading edge and combustion devices. Uniaxial tensile data were obtained for Laser Powder Bed Fusion of Haynes 230 at temperatures from 982 to 1177°C. The data is analyzed in terms of the strain rate sensitivity  $m$  and the stress dependence  $n$ . These two parameters are used to provide insight into the possible deformation mechanisms controlling plastic flow in this alloy over the temperature – strain rate range of interest. The values obtained suggest that under the present experimental conditions Haynes 230 deforms by a combination of dislocation slip and diffusion mediated recovery within the grain interior. Stress – strain curves exhibit oscillations suggesting the material is undergoing dynamic recrystallization during the tensile test. Optical imaging of the gage sections confirms the presence of dynamic recrystallization.

**E-8: Solidification and Crack Defect Formation on the Single Melt-track Scale for High  $\gamma'$  CoNi-base Superalloy Variants:** *Evan Raeker*<sup>1</sup>; Kira Pusch<sup>1</sup>; Kaitlyn Mullin<sup>1</sup>; James Lamb<sup>1</sup>; Ning Zhou<sup>2</sup>; Stephane Forsik<sup>2</sup>; Austin Dicus<sup>2</sup>; Michael Kirka<sup>3</sup>; Tresa Pollock<sup>1</sup>; <sup>1</sup>University of California, Santa Barbara; <sup>2</sup>Carpenter Technology Corporation; <sup>3</sup>Oak Ridge National Laboratory

Additive manufacturing enables the fabrication of complex part geometries, and is attractive for advanced aerospace components. Laser powder-bed fusion (LPBF), specifically, is being assessed for manufacturing structural components of gas turbine engines made from high-  $\gamma'$  volume fraction superalloys. However, the formation of crack defects during LPBF of nearly all superalloys within this class has undercut their mechanical performance greatly. This study builds on prior work examining the cracking susceptibility of high-  $\gamma'$  volume fraction superalloys during LPBF by simplifying the LPBF process down to single-track laser melting scans. The CoNi-base alloy GammaPrint-700 is utilized in this study, as the cracking resistance of the alloy can be controlled through the boron content. A means of improving the cracking resistance of the alloy through homogenization treatments prior to laser melting was identified. Characterization of the single-tracks reveals a possible mechanism of crack initiation via liquation cracking of grain boundaries in the substrate material, and propagation via solidification cracking along grain boundaries in the melt pool. Additionally, a protocol for assessing the cracking-resistance while developing new high-  $\gamma'$  volume fraction superalloys for additive manufacturing is discussed.

**E-9: Damage of Thermal Barrier Coated Superalloy Under Thermal Gradient Mechanical Fatigue:** Xin Zhan<sup>1</sup>; Dong Wang<sup>1</sup>; Guang Xie<sup>1</sup>; *Jian Zhang*<sup>1</sup>; <sup>1</sup>Institute of Metal Research

Thermal gradient mechanical fatigue (TGMF) tests were conducted on thermal barrier-coated (TBC) tubular specimens to investigate the damage behavior of the TBC under close-to-service conditions. Special attention was paid to the cracking behavior of TBC under TGMF tests with different temperature ranges, mechanical strain ranges and phase angles including in-phase (IP) and out-of-phase (OP) loading. Crack initiation, propagation, and coalescence within the ceramic top coat (TC) caused TBC failure during IP-TGMF tests with a 300-1000 °C temperature range and a mechanical strain range of 0.45% to 0.65%. Few cracks extend to the bond coat (BC) but did not further propagate into the substrate. Increasing the maximum temperature and mechanical strain range significantly changed the cracking behavior of these TBCs. Cracks run straight through the TC and BC followed by partial penetration into the substrate. The OP-TGMF loading shortened the TBC cycles to failure and accentuated the TBC damage, with separation occurring between TC and BC as well as between BC and substrate. Severe delamination at the thermally grown oxide (TGO)/BC interface results in premature TBC failure when the TBC system reaches a certain critical thickness of TGO.

**E-10: Effect of Free Surface, Oxide and Coating Layers on Rafting in  $\gamma'$ - $\gamma'$  Superalloys:** Wajih Jbara<sup>1</sup>; *Vincent Maurel*<sup>1</sup>; Kais Ammar<sup>1</sup>; Samuel Forest<sup>1</sup>; <sup>1</sup>Mines Paris - PSL University

Complex microstructure evolution has been observed both bare and coated Ni-based single crystal superalloys. Rafting and  $\gamma'$  depletion are investigated in this study through a brief experimental analysis and a detailed phase field model to account for mechanical-diffusion coupling. The proposed model has been implemented in a finite element code. As a main result, it is shown that rafting,  $\gamma'$  depletion close to free surface/oxide layer or  $\gamma'$  coalescence close to coating layer, and mechanical behavior are strongly coupled. The local additional flux of Al explains this coupling to a large extent. Finally, a discussion of strain localization and local flux of Al paves the way for clarification of these cases that degrade the performance of superalloys.

**E-11: In situ Observation of Initial Oxidation in Different Generations of Nickel-based Single-crystal Superalloys:** *Yunsong Zhao*<sup>1</sup>; <sup>1</sup>Beijing Institute of Aeronautical Materials

Due to the application of thermal barrier coatings, the concentrations of Cr in turbine blade alloys have been limited to low values (approximately 5 at.% or less) since the introduction of second-generation single-crystal superalloys. Thermal oxidation-induced rumpling and swelling of coating could lead to coating spallation and inner alloy failure, especially in advanced thin-wall turbine blades. The initial oxidized surface morphologies and elemental distributions were considered crucial to understanding the failure of superalloys. In this work, initial oxidation behavior in typical 1st- to 3rd-generation single-crystal superalloys was systematically studied in situ at nano-scale using an environmental transmission electron microscope from 20 - 800 oC. With increasing oxygen pressure, the oxide nucleated at the  $\gamma'/\gamma'$  interface, expanded along the  $\gamma$  channel and grew into the  $\gamma'$  phase. In thin foil samples, oxidation prompted the diffusion of base elements from the inner  $\gamma$  and  $\gamma'$  phases to the  $\gamma'/\gamma'$  interfaces in all alloys. With increasing Re content, the oxidation resistance decreased due to the evaporation of Re2O7 at the  $\gamma'/\gamma'$  interface in the 3rd-generation superalloy. This study provided technical guidance for optimizing the compositions of advanced single-crystal superalloys to enhance their oxidation resistance.

**E-12: Oxidation Behavior of Platinum-containing  $\gamma$ ,  $\gamma'$  and TROPEA Superalloy:** *Louis Hunault*<sup>1</sup>; Fernando Pedraza<sup>1</sup>; Jonathan Cormier<sup>2</sup>; Renaud Podor<sup>3</sup>; Stephane Mathieu<sup>4</sup>; <sup>1</sup>La Rochelle Université - LASIE UMR 7356 CNRS; <sup>2</sup>Institut Pprime; <sup>3</sup>ICSM; <sup>4</sup>Institut Jean Lamour

Platinum is used to form NiPtAl coatings and improve the oxidation/corrosion resistance of nickel-based superalloys operating under harsh conditions. The addition of 2 wt% (0.6 at%) Pt to the bulk composition of a single crystal nickel-based superalloy (TROPEA) markedly increased the mechanical properties at high temperature. However, the effects of Pt on the oxidation behavior of this new superalloy have never been studied, which is the main goal of this paper. TROPEA and model  $\tilde{a}$  and  $\tilde{a}'$  single phase alloys were thus oxidized at 950 °C in synthetic air. TROPEA reaches a parabolic regime only after 70 h of exposure. The establishment of an  $\tilde{a}$ -Al<sub>2</sub>O<sub>3</sub> protective layer is peculiarly delayed in comparison with the parent CMSX-4 superalloy according to literature. TROPEA forms a multilayer of oxides, including a continuous layer of (Ti<sub>x</sub>Ta<sub>1-x</sub>) O<sub>2</sub> during the transient period. It appears that Pt promoted the formation of this Ta-rich oxide. The Ta-rich oxide layer may play a role hindering the lowering of the PO<sub>2</sub> needed to selectively develop Al<sub>2</sub>O<sub>3</sub> scale or its presence just outlines the difficulty of TROPEA to develop the protective Al<sub>2</sub>O<sub>3</sub> scale in presence of platinum in the substrate. The 0.6 at% of Pt addition thus hampers the formation of a continuous and protective layer of  $\tilde{a}$ -Al<sub>2</sub>O<sub>3</sub> scale. In contrast, the model  $\tilde{a}$  and  $\tilde{a}'$  phases are prompt to develop an adherent and even scale of duplex Cr<sub>2</sub>O<sub>3</sub> + NiCr<sub>2</sub>O<sub>4</sub> and of  $\tilde{a}$ -Al<sub>2</sub>O<sub>3</sub> + NiO respectively, when oxidised at 950 °C in air for 100 hours.

**E-13: Stress Relaxation Testing as a High-throughput Method for Assessing Creep Strength in Laser Powder Bed Fusion Processed Ni-based Superalloys:** *Daniel McConville*<sup>1</sup>; Ben Rafferty<sup>2</sup>; Jeremy Iten<sup>2</sup>; Kevin Eckes<sup>2</sup>; Stan Baldwin<sup>2</sup>; Amy Clarke<sup>1</sup>; Jonah Klemm-Toole<sup>1</sup>; <sup>1</sup>Colorado School of Mines; <sup>2</sup>Elementum 3D

Ni-based superalloys processed by laser beam powder bed fusion (PBF-LB) additive manufacturing (AM) are ideal for high temperature structural applications in the aerospace and power generation industries due to the increased component complexity afforded by AM. However, conventional creep testing limits the rate at which new materials can be produced with AM. To help accelerate the acceptance of AM Ni-based alloys for high temperature applications, methods for high-throughput creep evaluation are needed. The stress relaxation test has potential to hasten the development and validation of PBF-LB Ni-based structural alloys by assessing a wide range of creep rates relevant to service conditions with a single test. In this work, alloy Ni230, a gas atomized powder derivative of Haynes 230, and variant thereof containing added TiC are assessed. Each material was subjected to a limited subset of conventional creep tests accompanied by stress relaxation tests. Following the calculation methodology described herein, stress relaxation tests predict creep rates and rupture times that align well with conventional creep test results. Stress relaxation tests also reveal features of microstructural characteristics and evolution which are not readily apparent with other experiments. Several advantages and challenges with stress relaxation testing are discussed.

**E-14: Surface-roughness Effects on Creep Performance In Ni-based Single-crystal Superalloys:** *Aidan O'Donnell*<sup>1</sup>; Pawan Chaugule<sup>1</sup>; Jean Briac Le-Graverend<sup>1</sup>; <sup>1</sup>Texas A&M University

Ni-based single-crystal superalloys must endure high temperature applications where creep is the main cause of failure. Coatings to protect against oxidation are not always applicable and oxidation should, therefore, be factored in. Thermogravimetric analyses were performed at 1000°C on René N4 to obtain the oxidation rate depending on the surface roughness. It was observed a strong non-linearity attributed to a transition between chemisorption and physisorption. The evolution of the oxidation rate was then phenomenologically modelled combining Lennard-Jones-type and Gaussian-type equations. The obtained expression was then implemented in a crystal-plasticity model used to predict the lifetime variation depending on the initial value of the surface roughness. The predicted lifetimes were then compared to the creep experiments at 1000°C/200 MPa. The evolution of the lifetime depending on the surface roughness match the evolution of the oxidation rate depending on the roughness and, therefore, the model predictions. Clearly, the results point to the importance of considering the contribution of surface roughness not only for fatigue loading but also to creep, which will allow to better understand creep-fatigue interactions.

**E-15: The Effect of Ti Replacement with Nb on the Long-term Oxidation Behaviour at High Temperatures of Ni-base Superalloys for Turbine Disc Applications:** Ana Carolina Silva<sup>1</sup>; Nabil Chaia<sup>2</sup>; Satoshi Utada<sup>3</sup>; Luciano Alkmin<sup>4</sup>; Gilberto Coelho<sup>1</sup>; Yuanbo Tang<sup>3</sup>; Roger Reed<sup>3</sup>; *Carlos Nunes*<sup>3</sup>; Phani Karamched<sup>3</sup>; <sup>1</sup>University of São Paulo; <sup>2</sup>Institut of Science & Technology, Federal University of Alfenas; <sup>3</sup>University of Oxford; <sup>4</sup>Federal Center of Technological Education Celso Suckow da Fonseca

This work focuses on the effect of partial and total replacement of Ti with Nb on the long-term oxidation at 800 °C up to ~2000 h of Ni-based superalloys for turbine disc applications. The replacement of Ti with Nb leads to a lower mass gain of the specimens, in both pseudo and isothermal oxidation conditions. The alloys presented a relatively smooth oxide scale surface; however, the roughness of the Nb-free/high-Ti alloy is twice of that of the Ti-free/high-Nb alloy. From XRD data, the Nb-free/high-Ti alloy presented Cr<sub>2</sub>O<sub>3</sub>, TiO<sub>2</sub>, Al<sub>2</sub>O<sub>3</sub>, (Ni,Co)Cr<sub>2</sub>O<sub>4</sub> and γ'+γ' (matrix) phases, while the Ti-free/high-Nb alloy presented Cr<sub>2</sub>O<sub>3</sub>, Al<sub>2</sub>O<sub>3</sub>, (Ni,Co)Cr<sub>2</sub>O<sub>4</sub>, γ'+γ' (matrix) and δ-Ni<sub>3</sub>Nb phases. The chromia layer thickness of the Ti-free/high-Nb alloy ranged from 1.0 to 1.5 μm, the thinnest among all the alloy for any given oxidation time and condition, with no mass change after approximately 280 h exposure. The exceptional oxidation behavior is attributed to the absence of Ti in this specific alloy composition. The semi-continuous alumina formation underneath the chromia scale as well as the formation of δ-Ni<sub>3</sub>Nb phase filling up the spaces between the alumina intrusions are probably the reason of delayed outward Cr diffusion.

**E-16: The Role of Silicon in the Protection Against Type I Hot Corrosion:** *Fernando Pedraza*<sup>1</sup>; D. Piel<sup>1</sup>; T. Kepa<sup>1</sup>; C. Gossart<sup>2</sup>; M. Mondet<sup>2</sup>; <sup>1</sup>Universite de La Rochelle; <sup>2</sup>Safran Aircraft Engines

Hot corrosion dramatically lowers the life of superalloy components by inducing pitting (Type II) or an extensive homogeneous attack (Type I), hence initiating cracks and decreasing the load bearing section. This degradation phenomena may occur in the coldest areas of high pressure turbine components but they are commonly found in the low pressure turbine parts like in the DS200+Hf nickel-based superalloy investigated in this work. Therefore, a Si-modified aluminide slurry coating was applied to the alloy, and its hot corrosion resistance was assessed under type I conditions with a Na<sub>2</sub>SO<sub>4</sub> deposit at various temperatures and times. The comparison against simple slurry aluminide with and without Si and out-of-pack aluminide coatings revealed for the first time in the literature that Si ties up W in the coatings thereby impeding acidic dissolution, which greatly improves the corrosion resistance of DS200+Hf superalloy. The W-free out-of-pack aluminide coating forms a protective alumina scale that delays the initiation of hot corrosion unless the coating is damaged. In contrast, the simple slurry aluminide coating without Si does not offer any protection in spite of the Cr segregation close to the surface.

## General Session 10: Additive Manufacturing II

Wednesday PM | September 11, 2024  
Exhibit Hall | Seven Springs Mountain Resort

**Session Chairs:** Nathalie Bozzolo, Safran; Stephane Forsik, Carpenter Technology Corporation

8:45 PM

**A Correlative In-situ, Ex-situ & 3D Analysis of Static Recrystallisation in a New Superalloy for 3D-printing:** *Yuanbo Tang*<sup>1</sup>; Anh Hoang Pham<sup>2</sup>; Satoshi Utada<sup>1</sup>; Jieming Zhang<sup>1</sup>; Yuhan Zhuge<sup>1</sup>; Shigekazu Morito<sup>2</sup>; Kazuto Arakawa<sup>2</sup>; D. Graham McCartney<sup>1</sup>; Roger Reed<sup>1</sup>; <sup>1</sup>University of Oxford; <sup>2</sup>Shimane University

By making particular use of high temperature confocal laser scanning microscopy, static recrystallisation is studied correlatively both in-situ and ex-situ in an as-fabricated superalloy made by laser-powder bed fusion (L-PBF). In this way, insights are gained into important recrystallisation phenomena with direct observations made – for the first time in this class of material – of phenomena such as nucleation of recrystallisation, subsequent grain growth, jerky flow of boundaries due to pinning and twin formation. The nucleation process – requiring strain-free lattice to be created by grain boundary migration – is visualised and its role in limiting the kinetics of recrystallisation is elucidated. Moreover, it is demonstrated that boundary mobility is initially prevented by Smith-Zener pinning due to a fine dispersion of secondary phases but also with a role played by solute drag caused by cellular micro-segregation. With increasing annealing time, the retarding pressure reduces due to carbide coarsening and/or dissolution as well as matrix compositional homogenisation, eventually allowing recrystallisation to take place. Further work will allow rich quantitative datasets to be gained which will allow for the testing of recrystallisation models.

9:10 PM

**Near Single-crystalline CMSX-4 Superalloy Builds with Laser-directed Energy Deposition (L-DED) using Model-informed Experiments:** *Swapnil Bhure*<sup>1</sup>; Divya Nalajala<sup>1</sup>; Abhik Choudhury<sup>1</sup>; <sup>1</sup>Indian Institute of Science

Manufacturing of single-crystalline Ni-base superalloy blades is extremely complex due to the intricate geometry of the blade profile and cooling channels. Additive manufacturing provides an excellent alternative to the classical Bridgman solidification, as it significantly reduces the number of steps involved. However, since the solidification conditions differ greatly, it is crucial to identify appropriate process parameters to ensure defect-free single-crystalline builds. In this paper, we present a complementary approach between experiments and numerical simulations of the melt pool shapes that enables the identification of the process parameter window for directional growth. Further, an incremental process optimization approach is developed that allows the gradual reduction of grains, creating conditions for epitaxial growth. Finally, it is revealed that the proposed strategy for achieving single-crystal growth conditions leads naturally towards crack-free builds of rods with the CMSX-4 alloy.



9:35 PM

**Eutectic Superalloys for Laser Powder Bed Fusion:** *Katerina Christofidou*<sup>1</sup>; Jonathon Markanday<sup>2</sup>; Alison Wilson<sup>2</sup>; Ed Pickering<sup>3</sup>; Nicole Church<sup>2</sup>; James Miller<sup>2</sup>; Nicholas Jones<sup>2</sup>; Neil Jones<sup>4</sup>; Howard Stone<sup>2</sup>; <sup>1</sup>University of Sheffield; <sup>2</sup>University of Cambridge; <sup>3</sup>University of Manchester; <sup>4</sup>Rolls-Royce

Due to the small freezing range of eutectic alloys, the Cotac-type alloys might be viable alternatives to conventional Ni-based superalloys when processed through additive manufacturing. Laser-pass assessment reveals that both Cotac-74 and Cotac-744 display improved cracking resistance when compared to the conventional Ni-based superalloy CM247LC. During laser powder bed fusion Cotac-74 displayed the highest cracking resistance, with no microcracking detected in the as-built or heat-treated microstructure. The promising results presented for Cotac-74 highlight the possible use of this alloy for the additive manufacturing of high-temperature aerospace components.

---

## General Session 11: Environmental Behavior and Coatings

Thursday AM | September 12, 2024  
Exhibit Hall | Seven Springs Mountain Resort

**Session Chair:** Ian Edmonds, Rolls-Royce Plc; Patrick Villechaise, CNRS

8:30 AM

**Comparison of the Effect of 2 at. % Additions of Nb and Ta on the 1100 °C Oxidation Behavior of Ni - 6Al - (4,6,8) Cr Model Alloys:** *Rafael Rodriguez De Vecchis*<sup>1</sup>; Rishi Pillai<sup>2</sup>; Kim Kisslinger<sup>3</sup>; Meng Li<sup>3</sup>; Judith Yang<sup>3</sup>; Brian Gleeson<sup>1</sup>; <sup>1</sup>University of Pittsburgh; <sup>2</sup>Oak Ridge National Laboratory; <sup>3</sup>Brookhaven National Laboratory

To continue improving alloy performance in harsh service environments, the development of alumina-forming nickel-based superalloys is essential. Current generations of these alloys heavily rely on the addition of refractory elements to enhance their mechanical properties at high temperatures; however, a systematic understanding of how such additions affect the overall oxidation behavior is still not well established, particularly from the standpoint of predicting the transition from internal to external alumina formation. The present work seeks to better understand the intrinsic effects that common minor additions of Ta and Nb have on the oxidation behavior of alumina-scale forming- $\gamma$  Ni model alloys. By combining a novel simulation approach with high-temperature oxidation experiments and advanced characterization techniques, the present study provides insightful details on the differing effects that 2 at. % addition of Ta and Nb have on the alumina-scale formation of Ni-based alloys during 1100 °C oxidation.

8:55 AM

**Fatigue Durability of a Single Crystal Nickel-based Superalloy with Prior Corrosion:** A. Martin<sup>1</sup>; E. Drouelle<sup>1</sup>; J. Rame<sup>2</sup>; *Fernando Pedraza*<sup>3</sup>; J. Cormier<sup>4</sup>; <sup>1</sup>Safran Aircraft Engines; <sup>2</sup>NAAREA; <sup>3</sup>Universite de La Rochelle; <sup>4</sup>Institut Pprime

The impact of hot corrosion on the low-cycle fatigue (LCF) life of the AM1 Ni-based single-crystal (SX) superalloy in as-cast (AC) and fully heat-treated (FHT) states has been studied. Microstructural features such as pores and chemical segregation have a significant impact on LCF fatigue strength at 950 °C. Surface pores act as stress concentration zones, influencing crack initiation and propagation. The reduction in the chemical dendritic segregation through solution heat treatment improves the LCF resistance. Pre-corrosion lowers the LCF lives by increasing stress concentration and facilitating multiple crack initiations with a brittle, spalled corrosion layer on the surface. The mechanical degradation occurs simultaneously to hot corrosion and oxidation, the latter being influenced by the distance from the layer undergoing hot corrosion. Heat treatment still appears to be a positive factor in improving the service life of AM1.

9:20 AM

**Influence of the Coating Brittleness on the Thermomechanical Fatigue Behavior of a -NiAl Coated R125 Ni-based Superalloy:** Capucine Billard<sup>1</sup>; Damien Texier<sup>2</sup>; Matthieu Rambaudo<sup>1</sup>; Jean-christophe Teissedre<sup>1</sup>; Dimitri Marquie<sup>3</sup>; Lionel Marcin<sup>3</sup>; Hugo Singer<sup>3</sup>; Noureddine Bourhila<sup>3</sup>; *Vincent Maurel*<sup>1</sup>; <sup>1</sup>Mines Paris - PSL University; <sup>2</sup>ICA Mines Albi; <sup>3</sup>SAE

The brittleness of an aluminide diffusion coating protecting a René 125 Ni-based polycrystalline superalloy was investigated over a wide range of temperatures in its as-received and thermally aged form. Isothermal and thermal cycled aging were performed on the coated system at a maximum temperature of 1100 °C. Microstructure evolutions and damage initiation within the coating were characterized. Interrupted tensile tests and thermomechanical fatigue tests were conducted to document critical stress-strain conditions leading to the coating cracking and lifetime for the case of thermo-mechanical fatigue loading. Advanced digital image correlation and acoustic emission techniques were used to detect coating cracking. Isothermal oxidation or cyclic oxidation led to improved strain-to-failure due to metallurgical evolutions and also longer fatigue life under thermomechanical fatigue conditions.

9:45 AM

**Very High Cycle Fatigue Properties of a Coated Nickel-based Single Crystal Superalloy:** *Antonio Vicente Morales*<sup>1</sup>; Florent Mauget<sup>2</sup>; Amélie Caradec<sup>2</sup>; Baptiste Larrouy<sup>3</sup>; Patrick Villechaise<sup>2</sup>; Jonathan Cormier<sup>2</sup>; <sup>1</sup>Safran Helicopter Engines and Institut Pprime; <sup>2</sup>Institut Pprime; <sup>3</sup>Safran Helicopter Engines

Very High Cycle Fatigue (VHCF) properties of thermally sprayed MCrAlY coated samples of CMSX-4 at high temperature were studied. Nine fatigue tests up to failure were performed at 1000 °C, 20 kHz and R = -1 on coated samples. These samples showed lower fatigue life when compared with the bare reference. Fatal crack initiation systematically occurred at the interdiffusion zone (IDZ) between the coating and the CMSX-4 substrate or at a casting pore in the vicinity of the IDZ. Failed samples showed a high density of secondary surface cracks. In order to better understand the mechanism leading to surface cracking, one interrupted test was performed. It is shown that cracks nucleated from the very first fatigue cycles and propagated through the coating almost instantly. Surface cracks then spent most of the fatigue lifetime sitting at the IDZ/substrate interface. The fatal as well as the surface crack initiation mechanisms are discussed to better understand the durability in these VHCF conditions.

---

**General Session 12: Disk Alloy Mechanical Behavior III**

Thursday AM | September 12, 2024  
Exhibit Hall | Seven Springs Mountain Resort

**Session Chairs:** Michael Mills, Ohio State University; Jonathan Cormier, ENSMA - Institut Pprime - UPR CNRS 3346

---

**10:30 AM**

**Modeling Microstructural Development During Hot Working of Ni-based Superalloy 680:** *Jose Gonzalez Mendez*<sup>1</sup>; Will Heffern<sup>2</sup>; Spencer Hagaman<sup>2</sup>; Matias Troper<sup>2</sup>; Victoria Tucker<sup>2</sup>; Austin Dicus<sup>1</sup>; Mario Epler<sup>1</sup>; Matthew Krane<sup>2</sup>; Mike Titus<sup>2</sup>; Stephane Forsik<sup>1</sup>; <sup>1</sup>Carpenter Technology; <sup>2</sup>Purdue University

In this work, dynamic recrystallization kinetics for a nickel alloy are characterized during hot deformation. Gleeble compression testing within a temperature range from 927 °C to 1149 °C is employed to replicate typical forging conditions with strain rate varying from 0.1 s<sup>-1</sup> to 10 s<sup>-1</sup>. Microstructural and flow stress results were analyzed via the Johnson-Mehl-Avrami-Kolmogorov (JMAK) model that describes the mechanisms triggering recrystallization during forging operations. This model considers the significant variables of hot deformation such as temperature, strain, strain rate, and initial structure. The developed model illustrates the dynamic recrystallization fraction and dynamically recrystallized grain diameter within defined temperature ranges based on the JMAK configuration. Results indicate that deformation above 1093 °C yields high dynamic recrystallization. Conversely, at lower temperatures grain structure is highly dependent on strain and strain rate. Validation tests coupling Gleeble compression tests and FE modeling comparisons covering the forging conditions are included in this study.

**10:55 AM**

**Microstructurally Informed Material Model for Haynes® 282:** *Monica Soare*<sup>1</sup>; Vito Cedro III<sup>2</sup>; Vipul Gupta<sup>1</sup>; Mallikarjun Karadge<sup>1</sup>; Reddy Ganta<sup>3</sup>; <sup>1</sup>GE Research; <sup>2</sup>National Energy Technology Laboratory; <sup>3</sup>The Energy Industries of Ohio

The precipitation strengthened alloy Haynes® 282 possesses very good strength, creep resistance and corrosion resistance at high temperatures. It is one of the best candidates for a range of high temperature components for next generation of power systems as Advanced Ultra-Supercritical (A-USC) boilers and steam turbines, Supercritical carbon dioxide (sCO<sub>2</sub>) power cycles as well for aerospace gas turbine parts (combustor lines, nozzles, exhaust sections). Some of these components operate for very long time (30-40 years) during which they are subjected to high temperature (up to 60% of the Liquidus Temperature, T<sub>m</sub>) creep as well as cyclic loading (cyclic temperature and stress variations). Assessing long term material behavior through combined accelerated testing and model predictions, is an important step in the material qualification process. Towards this goal, a material constitutive model was developed capturing long term creep as well as cyclic plasticity, with and without hold time at two temperatures: 593 °C and 760 °C. The model was calibrated on creep and low cycle fatigue tests performed on smooth specimens. The model predictions were compared with experimental data performed on smooth circular and on notched specimens, in terms of stress-strain response and number of cycles to failure.

**11:20 AM**

**Cyclic- and Dwell-fatigue Crack Growth Behavior in a Phase Transformation Strengthened Disk Superalloy:** *Christopher Kantzos*<sup>1</sup>; Timothy Smith<sup>1</sup>; Jack Telesman<sup>2</sup>; Ian Dempster<sup>3</sup>; Timothy Gabb<sup>1</sup>; <sup>1</sup>NASA Glenn Research Center; <sup>2</sup>HX5 LLC; <sup>3</sup>Wyman Gordon

A follow-on study was performed on NASA's recently developed Nickel-based P/M TSNA-1 disk alloy to evaluate the influence of processing on the alloy's mechanical properties. The composition of the alloy was tailored to improve the high temperature creep strength through transformation strengthening of precipitate phases. Initial alloy development was done utilizing HIP processing. The follow-on study evaluated the properties of the forged version of the alloy which provided for a more realistic processing history similar to that utilized in the engine industry. The creep performance of the forged material significantly exceeded the original HIP material, and outperformed alloys like LSHR and ME3 by an order of magnitude. The TSNA-1 alloy's cyclic and dwell FCG behavior was also characterized. While the HIP condition the alloy exhibited very poor dwell FCG resistance in comparison to the LSHR P/M disk alloy, the forging processed TSNA-1 drastically improved the crack growth behavior. In the forged condition both cyclic and dwell FCG behavior of the alloy were equivalent to a current LSHR P/M alloy.

**11:45 AM**

**Formation of the  $\gamma''$ -Ni<sub>2</sub>(Cr, Mo, W) phase during a two-step aging heat treatment in HAYNES® 244® Alloy:** *Thomas Mann*<sup>1</sup>; Victoria Tucker<sup>2</sup>; Peter Kenesei<sup>3</sup>; Jun-Sang Park<sup>3</sup>; Reza Roumina<sup>4</sup>; Emmanuelle Marquis<sup>4</sup>; Michael Fahrman<sup>1</sup>; Michael Titus<sup>2</sup>; <sup>1</sup>Haynes Intl.; <sup>2</sup>Purdue University; <sup>3</sup>Argonne National Laboratory; <sup>4</sup>University of Michigan

Precipitation hardening is the dominant method of achieving high strength in most Ni-based superalloys. The formation of nanoscale precipitates during thermal exposure is often studied to determine the optimal methods of attaining high strength. The commercial Ni-based superalloy, HAYNES® 244® alloy, is strengthened through a novel  $\gamma''$ -Ni<sub>2</sub>(Cr,Mo,W) intermetallic phase that forms during a two-step aging cycle. The precipitation kinetics of this intermetallic  $\gamma''$  phase are sluggish for single-step aging in comparison to the  $\gamma''$  phase in precipitation strengthened Ni-based alloys, but a two-step aging treatment has shown to reliably harden the alloy and improve high temperature properties compared to a single-step aging heat treatment. To investigate the formation and coarsening of this phase, heat treated samples of the 244 alloy were analyzed with high energy in situ and ex situ X-ray techniques such as small angle X-ray scattering and wide angle X-ray scattering as well as Vickers microhardness, electron microscopy, and atom probe tomography. The relationship between hardness, aging parameters, and microstructure evolution are discussed. The enthalpy of formation and precipitate solvus temperature were determined with high temperature differential scanning calorimetry and dilatometry analysis.

<b>A</b>		
Albert, T. ....	14	
Albrecht, R. ....	14	
Alkmin, L. ....	24	
Al-Kotob, M. ....	8	
Almirall, N. ....	17	
Ammar, K. ....	22	
Anahid, M. ....	20	
Antonov, S. ....	6	
Arakawa, K. ....	24	
Arciniaga, L. ....	2, 18	
<b>B</b>		
Backes, G. ....	17	
Baldwin, S. ....	23	
Baler, N. ....	21	
Balila, N. ....	22	
Bandorf, J. ....	6	
Barot, L. ....	18	
Bartsch, M. ....	16	
Baudequin, X. ....	8	
Bender, M. ....	3	
Bennett, J. ....	17	
Bergamaschi, E. ....	6	
Bernacki, M. ....	19, 20	
Bertheau, D. ....	7	
Bezold, A. ....	3, 12, 14	
Bhadeliya, A. ....	16	
Bhure, S. ....	24	
Bignon, M. ....	19	
Billard, C. ....	25	
Black, R. ....	10	
Blaizot, J. ....	17, 19, 20	
Boettger, B. ....	16	
Bordas, R. ....	18	
Borovikov, V. ....	3	
Bortoluci Ormastroni, L. ....	13, 15	
Bourhila, N. ....	25	
Bozzolo, N. ....	17, 19, 20, 24	
Breneman, R. ....	15	
Brodin, H. ....	21	
Burlatsky, S. ....	20	
Burow, J. ....	21	
<b>C</b>		
Caradec, A. ....	7, 25	
Caron, P. ....	13	
Cedro III, V. ....	26	
Cernatescu, I. ....	15	
Cervellon, A. ....	5, 18	
Chabrier, A. ....	17	
Chaia, N. ....	24	
Chatterjee, S. ....	21	
Chaugule, P. ....	23	
Chen, S. ....	10	
Chen, T. ....	7	
Chen, Z. ....	11	
Choudhury, A. ....	24	
Christofidou, K. ....	20, 25	
Church, N. ....	20, 25	
Clarke, A. ....	23	
Cody, D. ....	5	
Coelho, G. ....	24	
Colombo, G. ....	4, 21	
Connolly, E. ....	21	
Connor, L. ....	20	
Cormier, J. ....	2, 5, 7, 8, 13, 14, 15, 18, 23, 25, 26	
Cosquer, Y. ....	5	
Coyne-Grell, A. ....	19	
Cui, Y. ....	4	
<b>D</b>		
Dade, M. ....	17	
Dalpia, G. ....	13	
de Jaeger, J. ....	20	
De Jaeger, J. ....	7, 17	
de Miranda, H. ....	13	
Dempster, I. ....	26	
Dendievel, R. ....	21	
Dennstedt, A. ....	16	
Detroit, M. ....	6	
Dicus, A. ....	20, 21, 22, 26	
DiDomizio, R. ....	5	
Dörries, K. ....	21	
Drouelle, E. ....	25	
D'Souza, N. ....	20	
Duan, R. ....	7	
Dumont, C. ....	17, 19, 20	
<b>E</b>		
Echlin, M. ....	20	
Eckes, K. ....	23	
Edmonds, I. ....	2, 11, 25	
Egan, A. ....	3	
Elcrin, T. ....	21	
Epler, M. ....	4, 21, 26	
Eyidi, D. ....	15, 18	
<b>F</b>		
Fage, M. ....	17	
Fahrmann, M. ....	8, 26	
Fedelich, B. ....	16	
Feng, L. ....	3	
Feng, Q. ....	6, 12, 13, 14	
Finet, L. ....	17	
Fleck, M. ....	9	
Flipon, B. ....	20	
Forest, S. ....	22	
Fornara, A. ....	17	
Forsik, S. ....	20, 21, 22, 24, 26	
Fortunier, R. ....	18	
Franchet, J. ....	20	
Froeliger, T. ....	21	
Furrer, D. ....	15, 20	
Futoma, M. ....	18	
<b>G</b>		
Gabb, T. ....	26	
Galindo-Nava, E. ....	9	
Galy, D. ....	20	
Ganta, R. ....	26	
Gao, Y. ....	22	
Gehrmann, B. ....	21	
Georges, E. ....	17	
Gillet, S. ....	18	
Glatzel, U. ....	9	
Gleeson, B. ....	25	
Glover, N. ....	2	
Goeken, M. ....	6	
Göken, M. ....	12, 14	
Gonzalez Mendez, J. ....	26	
Gossart, C. ....	24	
Govaere, A. ....	8	
Grandjean, B. ....	12	
Gray, S. ....	11	
Gregson, S. ....	2	
Guo, H. ....	5	
Guo, J. ....	16	
Gupta, V. ....	17, 26	
Gu, Y. ....	5	
<b>H</b>		
Haberland, C. ....	21	
Hagaman, S. ....	26	
Hale, C. ....	18	
Hanlon, T. ....	5, 17	
Han, Q. ....	11	
Harada, H. ....	4, 12	
Hardy, M. ....	2, 4, 6, 19	
Harikrishnan, R. ....	11	
Hasselqvist, M. ....	11	
Hatzoglou, C. ....	17	
Hausmann, A. ....	6	
Hausmann, L. ....	6	
Hayashi, M. ....	8	
Hecker, L. ....	12	
Heffern, W. ....	26	
Hemes, S. ....	17	
He, S. ....	13	
Horie, T. ....	12	
Hou, M. ....	6	
Hryha, E. ....	21	
Huiwei, L. ....	8	
Hunault, L. ....	23	
Hung, C. ....	6	
Huyghe, T. ....	17	
<b>I</b>		
Ikeda, A. ....	4	
Imano, S. ....	8	
Ionov, I. ....	4	
Iten, J. ....	23	

Izumi, T	8	Li, J	5	<b>N</b>	
<b>J</b>		Li, L	6, 7, 10, 12, 13, 14	Nagel, O	12
Jablonski, P	6	Li, M	25	Nait-Ali, A	8, 18
Jankowski, J	3	Li, S	4	Nakayama, A	9
Jbara, W	22	Liu, K	7	Nalajala, D	24
Jiang, Z	12	Liu, Z	16	Neumeier, S	3, 6, 12, 14
Jokisch, T	16	Li, Y	5, 12, 19	Nguyen, C	19, 20
Jones, N	4, 20, 25	Locq, D	5, 21	Nicolaus, M	16
Jullien, M	10	Longfei, L	8	Nouveau, S	19
<b>K</b>		Longuet, A	8	Nunes, C	9, 24
Kamal, M	20	López Galilea, I	12, 16	<b>O</b>	
Kammermeier, E	4	Lorcharoensery, K	17	O'Connell, C	15
Kang, M	19	Lunt, A	21	O'Donnell, A	23
Kang, Y	7	Lu, S	6, 13, 14	Ohmura, T	15
Kantzos, C	26	Lu, Y	16	Olbricht, J	16
Karadge, M	26	<b>M</b>		Orlacchio, F	19
Karamched, P	24	Machado Alves da Fonseca, F	7, 15	Osada, T	4, 15
Karpstein, N	3, 14	Maezawa, H	12	Osawa, M	4
Kawagishi, K	4, 12, 13, 15	Mann, T	8, 26	Owen, L	9
Kenesei, P	26	Mansoz, B	13	<b>P</b>	
Kepa, T	24	Marcin, L	25	Paes, M	13
Kirchmayer, A	12	Markanday, J	20, 25	Panella, M	16, 18
Kirka, M	22	Marquie, D	25	Pang, H	4, 6
Kirzinger, A	6	Marquis, E	26	Park, J	26
Kisslinger, K	25	Martin, A	25	Patil, S	17
Kittel, J	17	Mathieu, S	23	Payton, E	18
Klemm-Toole, J	23	Matsuoka, H	11	Pedersen, M	17
Koch, R	15	Mauget, F	25	Pedraza, F	16, 23, 24, 25
Kohata, T	4	Maurel, V	22, 25	Pelliccione, C	15
Kollapalli, I	21	Mazor, A	17	Peng, P	19
Kontis, P	2, 5, 17	McCartney, D	24	Perez, M	17
Körner, C	4	McConville, D	23	Pérez, M	19
Krane, M	26	McLasky, C	17	Perrut, M	5
Krutz, N	17	Mellier, D	7	Pettinari-Sturmel, F	13
Kueppers, W	17	Mendelev, M	3	Pham, A	24
Kwiatkowski da Silva, A	13	Menou, E	5	Pickering, E	25
<b>L</b>		Meshkov, A	5	Piegert, S	21
Lambert, R	8	Michalik, S	20	Piel, D	24
Lamb, J	20, 22	Mignanelli, P	4	Pillai, R	25
Laplanche, G	3	Miller, J	9, 20, 25	Pino Munoz, D	17, 19
Larrouy, B	25	Miller, V	18	Pirch, N	17
Lasne, C	8	Mills, M	3, 26	Pitchforth, J	20
Lawson, J	3	Miná, É	13	Podor, R	23
Leblanc, J	8	Minet-Lallemand, K	21	Polato lu, C	11
Lee, Y	18	Miquel, M	11	Pollock, T	20, 22
le Graverend, J	11	Mitchell, I	2	Prié, M	8
Le-Graverend, J	23	Miura, H	9	Pusch, K	20, 22
Legros, M	10	Moehwald, K	16	<b>Q</b>	
Lenz, M	3	Mondet, M	24	Qiang, F	8
Le Sache, L	17	Morito, S	24	<b>R</b>	
Le Saché, L	20	Mori, Y	4, 8	Rae, C	6, 9, 11
Li, A	11	Motta, M	13	Raeker, E	20, 22
Liang, J	4	Müller, B	17		
Liebscher, C	13	Müller, M	9		
Li, H	10	Mullin, K	22		
		Murakami, H	7		

Rafferty, B	23
Rambaudon, M	25
Rame, J	5, 13, 15, 25
Ramsperger, M	4
Rapetti, A	5
Reed, R	9, 11, 15, 24
Rehmer, B	16
Reker, D	16
Remichi, R	17
Reppold, R	13
Rodriguez De Vecchis, R	3, 25
Roebuck, B	20
Rösler, J	21
Roumina, R	26
Rowlands, B	9
<b>S</b>	
Saboundji, A	5
Saito, T	4
Sakaguchi, M	11
Sallot, P	7
Saly, E	7
Sasaki, R	9
Sasakura, I	11
Sattari, M	21
Saunders, E	11
Sazerat, M	18
Schleifer, F	9
Schwalbe, C	11, 16, 18
Seetharaman, V	15
Seidel, F	16
Severs, K	18
Shah, N	22
Shaikh, A	21
Shao, Y	14
Shen, X	9
Shen, Z	7
Shibayama, T	8
Shukla, A	5
Signor, L	7
Silva, A	24
Silva, C	13
Silva, R	13
Singer, H	25
Sirrenberg, M	12
Skrotzki, B	16
Smith, T	3, 6, 20, 26
Soare, M	26
Soares Janeiro, I	19
Somsen, C	21
Song, L	8
Song, W	9
Sowa, R	16
Spiecker, E	3, 14
Srinivasan, D	21, 22
Srisuriyachot, J	21
Stinville, J	10
Stolz, S	15

Stone, H	4, 6, 9, 10, 20, 25
Sun, X	5
Sutter, N	8
Suzuki, A	5, 16
Suzuki, K	9
Suzuki, S	4, 11, 12, 15

## T

Tabata, C	12, 15
Takata, Y	12
Tancret, F	5
Tang, Y	9, 11, 20, 24
Tan, Z	5
Teissedre, J	25
Telesman, J	26
Texier, D	10, 25
Thome, P	2, 18
Thuvander, M	21
Tian, Q	7
Tillmann, W	16
Tin, S	2, 18, 19
Titus, M	8, 26
Toda, Y	7
Toualbi, L	21
Troper, M	26
Tsankova, S	12
Tucker, V	26

## U

Utada, S	9, 11, 19, 24
----------	---------------

## V

Van Weereld, F	4
Vicente Morales, A	25
Villechaise, P	7, 13, 18, 25
Violatos, I	19

## W

Wahlmann, B	4
Wang, B	4
Wang, D	22
Wang, J	4, 19
Wang, R	9
Wang, T	21
Wang, X	5
Wang, Y	3
Weber, S	12, 16
Weidinger, J	4
Wilson, A	25
Wise, G	4
Woolrich, J	11
Wossack, I	13
Wu, A	8
Wu, M	3, 14
Wu, P	7

## X

Xiaoli, Z	8
Xiaorui, Z	8
Xia, S	16
Xia, W	5
Xie, G	12, 22
Xinli, W	8

## Y

Yadav, R	22
Yang, J	25
Yang, S	10
Yeh, A	7
Yokokawa, T	4, 12, 15
Yoshimoto, S	8
Yue, Q	5
Yuyama, M	12

## Z

Zehl, R	3
Zenk, C	4, 6
Zhang, B	7, 10
Zhang, J	7, 12, 13, 16, 22, 24
Zhang, Q	11
Zhang, W	7, 10
Zhang, X	6
Zhang, Z	5, 19
Zhan, X	22
Zhao, X	5
Zhao, Y	13, 23
Zheng, L	18
Zheng, W	14
Zhou, N	4, 20, 21, 22
Zhou, Y	4, 5
Zhuge, Y	24
Zou, M	6